CHAPTER 3

EXPERIMENTAL AND PRELIMINARY INVESTIGATION

3.1 Instrument geometry

3.1.1 Oscillation camera and photographs

The camera that we use to take the oscillation photograph is the Weissenberg camera shown in Fig.3.1.1. It has the cylindrical shape with the diameter of 57.3 mm. X-ray films are held in the form of a cylinder and protected by a black paper envelope. The design of this envelope depends on the general camera used.
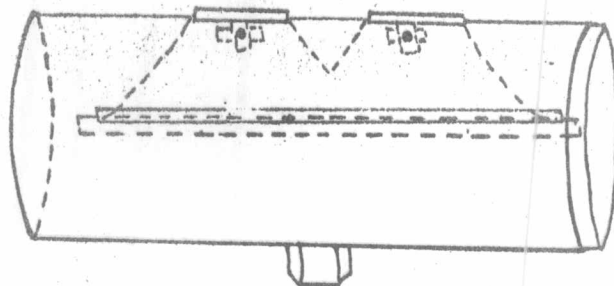

Fig.3.1.1 Cylindrical camera.

The specimen holder used for this camera is a goniometer head as shown in Fig.3.1.2 ; it has two arcs which are perpendicular to each other, centered at the crystal, and

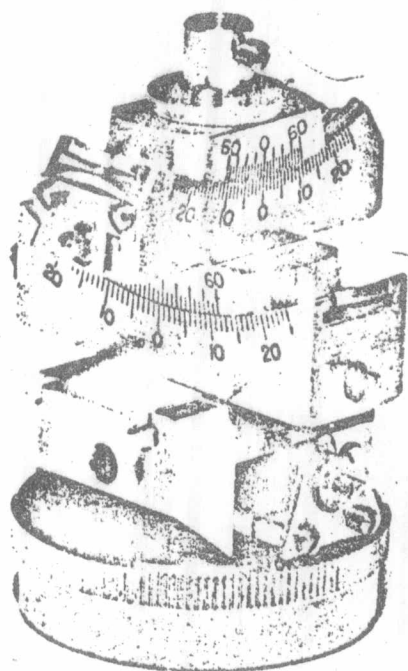allow the crystal to be tipped $\pm 20^{\circ}$ in each of two planes

Fig.3.1.2 Goniometer head

The crystal is glued to a suitable glass fibre and this is attached to the top of the goniometer head which is fastened by means of a threaded ring to the spindle of the camera. So the crystal is fixed with respect to the spindle and the adjustable azimuth scale.

For the oscillation method, the crystal is oscillated by a small motor in a suitable range, while the X-ray beam is directed onto the crystal through a metal collimator perpendicular to the rotation axis of the crystal.

When the crystal has been properly mounted, the direct beam stop is slid into place next to the rotation spindle. This stop serves to prevent the direct beam from striking the camera. The film holder is then attached to its base, which is shifted until the crystal is located about the middle of the

film and then locked in place.   The collimator is put into
position and the movable base is translated until the opening
of the collimator is in line with the beam from the tube.

The camera motor is turned on, the X-ray tube
started, and the shutter on the tube opened.

From Fig.3.1.3a, the reflected beams are located
on the imaginary cones the axes of which coincide with the
rotation axis.   These cones intersect the cylindrical film in
a series of circles.   After the exposed film is developed,
fixed and washed, the diffraction pattern is found to lie on a
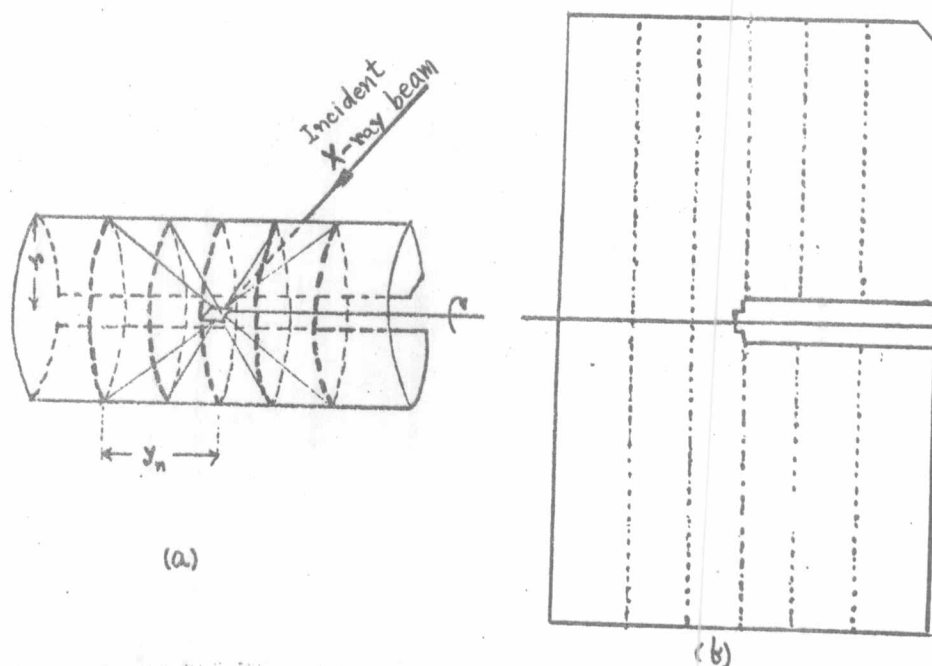series of straight lines, called layer lines, as in Fig.3.1.3b.

(a)

(b)

Fig.3.1.3a. The reflecting beam on   b. The layer lines on an
       the cylindrical film.   oscillation photograph.

The length of the rotation axis can be computed
from an experimentally determined cone angle, the geometry of the
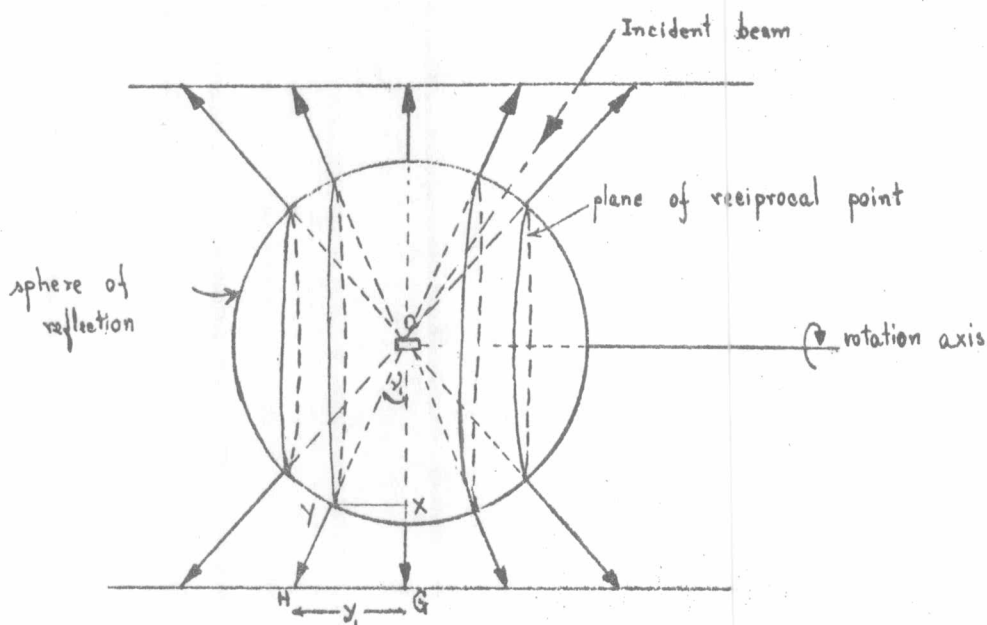apparatus, and the locations of the layer lines.

Fig.3.1.4 The relation of the angle ν and the layer

lines on an oscillation photograph.

In Fig.3.1.4, ψ is the angle subtended by the cone

onto the horizontal axis , the angle ν_1 for the first layer cone

is

$$\sin \nu_1 \;=\; \frac{XY}{OY}$$

If the rotation axis is c $[001]$, $XY = d^{*}_{001}$, the distance

between two reciprocal planes. In terms of the direct lattice, for the

orthogonal axes system

$$d^{*}_{001} \;=\; \frac{\lambda}{c}$$

where λ is the wavelength of the X-ray beam

and   c   is the length of the rotation axis.

when   OY   is the radius of the reflecting sphere, λ , so

$$\sin \nu_1 \;=\; \frac{\lambda}{c}$$

for the nth layer line,

$$\sin \nu_n = \frac{n \lambda}{c} \qquad \ldots (3.1.1)$$

The distance between the zero and first layer lines as measured on the film is y_1. Then

$$\tan \nu_1 = \frac{HG}{OG} = \frac{y_1}{r}$$

where $OG = r$ is the radius of the cylindrical film.

At a height y_n, the nth layer line is given by

$$\tan \nu_n = \frac{y_n}{r}$$

for which

$$\nu_n = \tan^{-1} \frac{y_n}{r} \qquad \ldots (3.1.2)$$

Substituting ν_n in (3.1.1) gives the length of the rotation axis

$$c = \frac{n \lambda}{\sin\{\tan^{-1}(y_n/r)\}} \qquad \ldots (3.1.3)$$

By rotating a crystal in an X-ray beam about each of its axes and measuring the identity periods along the layer lines the lengths of the cell edges along these directions are measured.

3.1.2 Weissenberg camera and photographs

Each reflection in the Weissenberg photograph is associated with a reciprocal lattice point of the crystal. The plane surface of a photographic film is two-dimensional, and

can record two co-ordinates.   With c as the rotation axis, every
spot on the zero layer film bears an index of the type hk0.   If
the first layer is recorded, then every spot on the film will
bear an index of the type hk1, and so on.

        A layer-line screen used with the Weissenberg
camera, is a cylinder with an equatorial slit.   It is inserted
between the crystal and the film to permit only one diffraction
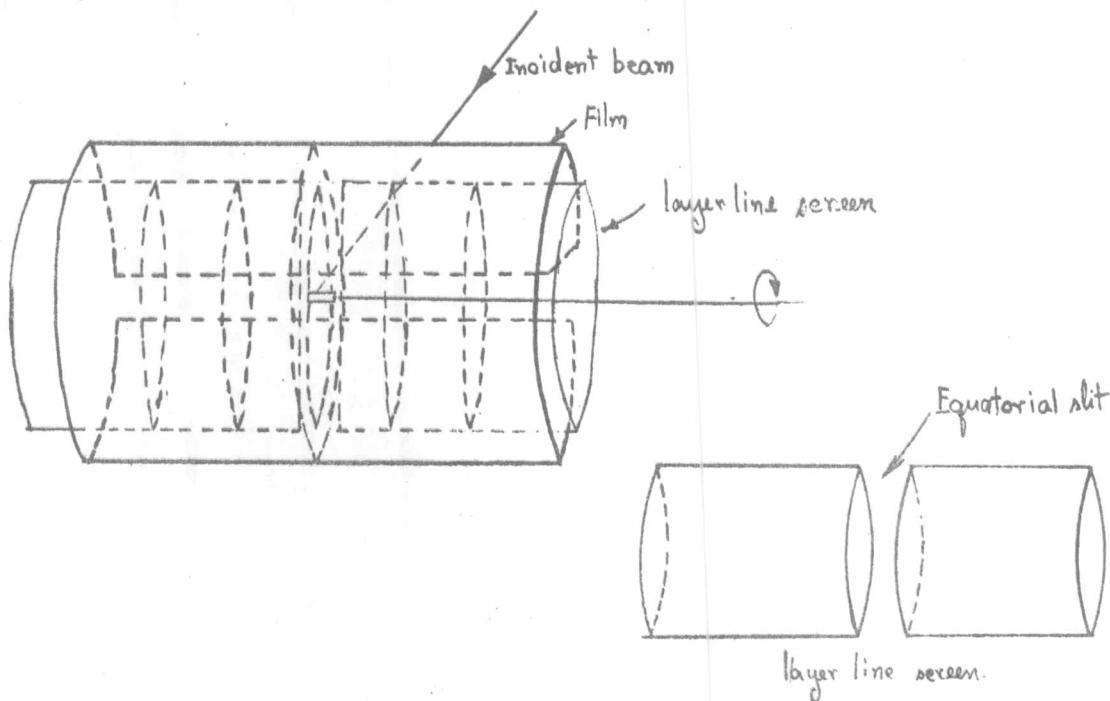cone to reach the film, see Fig.3.1.5.

Fig.3.1.5 Weissenberg apparatus.

        During the oscillation of the crystal in the range
of 200°- 220°, the film can be moved synchronously along the
rotation axis.   The reflections on the film are spread across
the film and form a two-dimensional pattern.

        The diagram of the motion of the camera in the
Weissenberg method is shown in Fig.3.1.6.

Motion of film

Film

$\omega = 0°$

$\omega = 45°$

$\omega = 90°$

$\omega = 135°$

$\omega = 180°$

$\omega = 220°$

Motion of film

Film

$\omega = 0°$

$\omega = 45°$

$\omega = 90°$

$\omega = 135°$
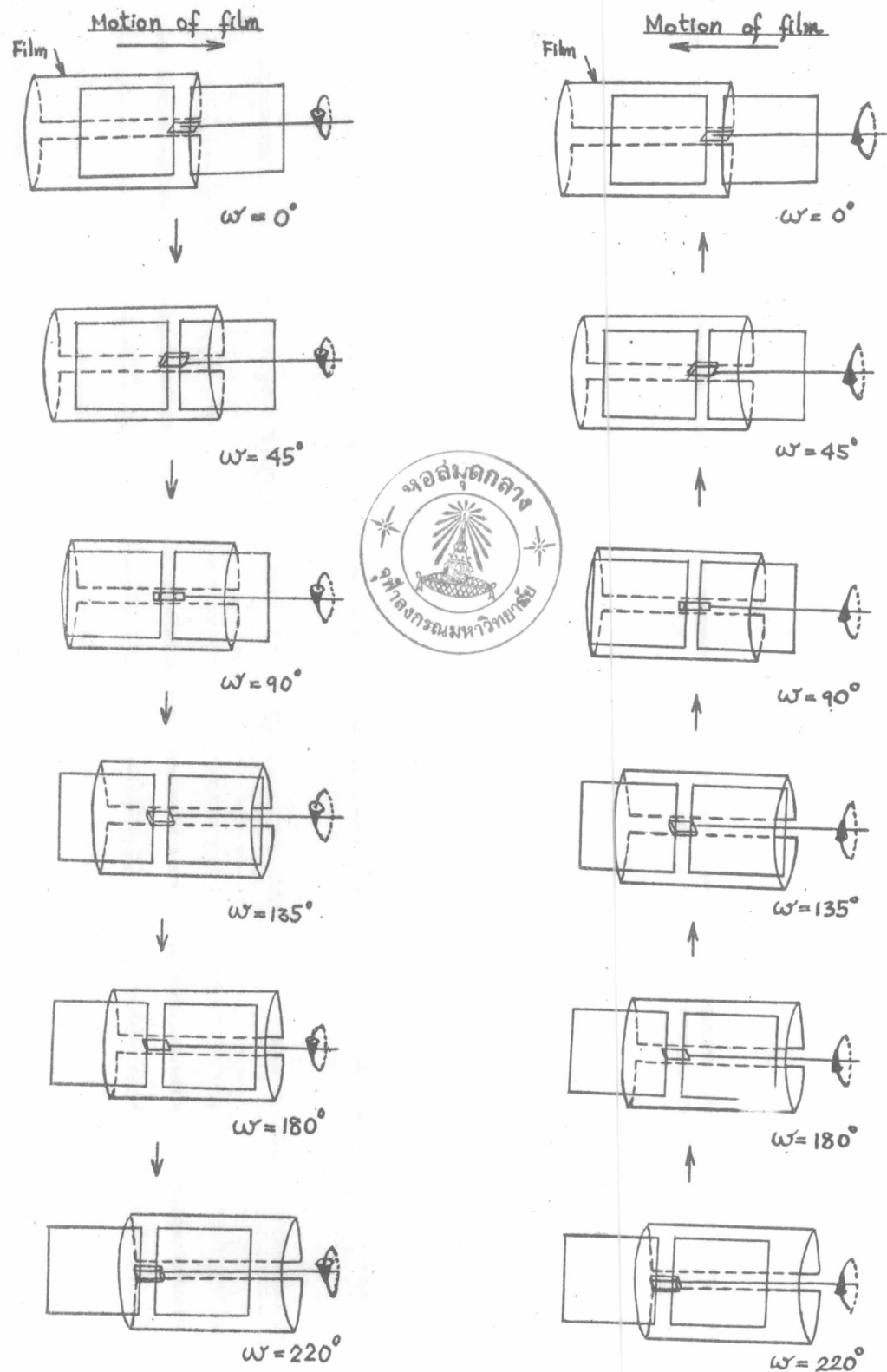
$\omega = 180°$

$\omega = 220°$

Fig.3.1.6 The motion of the camera for a 220°
oscillation in a Weissenberg camera.

The reciprocal lattice may be described as a series
of levels, which are normal to and spaced at equal intervals
along the rotation axis, that passes through the origin of the
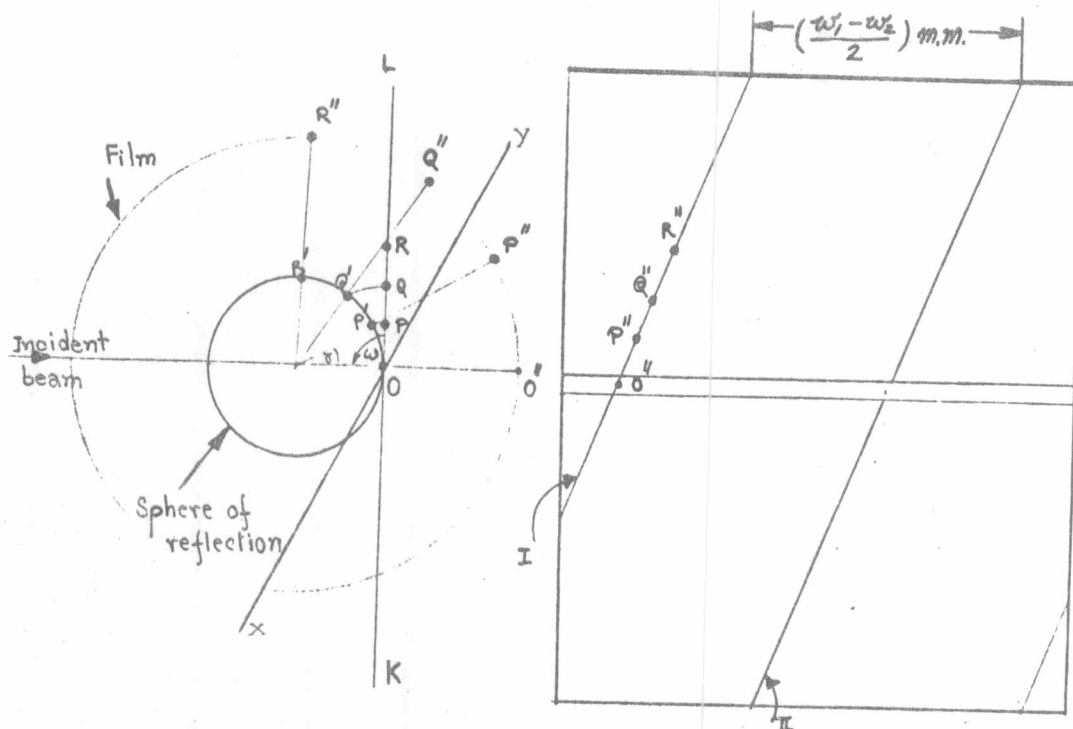reciprocal lattice.

Fig.3.1.7 The projection of the central line KL which appears
as a line in a zero-level Weissenberg photograph.

Consider Fig.3.1.7 which represents the row of
reciprocal lattice points in the sphere of reflection.   The
reciprocal lattice point P is in the zero layer.   Th reflection
can be produced when the crystal is rotated into such a position
that the reciprocal lattice point moves to P'.   A Weissenberg
photograph is regarded as a projection of the reciprocal lattice.

One reflection hkl is formed when the correspond-
ing reciprocal lattice point, hkl, rotates through the circle of
reflection.

The azimuth angle of reflection, τ , and a rotation angle, ω , may be described as the reflection co-ordinates of the reciprocal point on the film.   The following relation

$$\tau \quad = \quad 2\omega$$

holds for every position of the line KL in Fig.3.1.7, as it rotates through the sphere.

As the crystal rotates in the path of the beam , each crystal row in the level rotates in turn through the sphere and generates reflections which lie on a lattice line projection. In Fig.3.1.7(b) two rows I and II, are separated by an angle $(\omega_1 - \omega_2)$.   In the interval, the film translates $(\omega_1 - \omega_2)/2$ mm. if the translation constant of the Weissenberg instrument is 1 mm./2^0

Noncentral rows do not intersect the rotation axis. In Fig.3.1.8 shows the curves represented by a central and non-central lines, rotates through 180^0 in the path of the X-ray beam.

The zero level is recorded with the X-ray beam directed at right angles to the rotation axis.   In the upper level photographs, the incident X-ray beam and the diffracted beam make the same angle with the rotation axis as illustrated in Fig.3.1.9, the angle between the incident beam and the axis is called the inclination angle, μ , and is given by

$$2a\cos\mu \quad = \quad h\lambda \qquad \ldots (3.1.4)$$

where   a is the length of the crystal axis,

h is an integer,

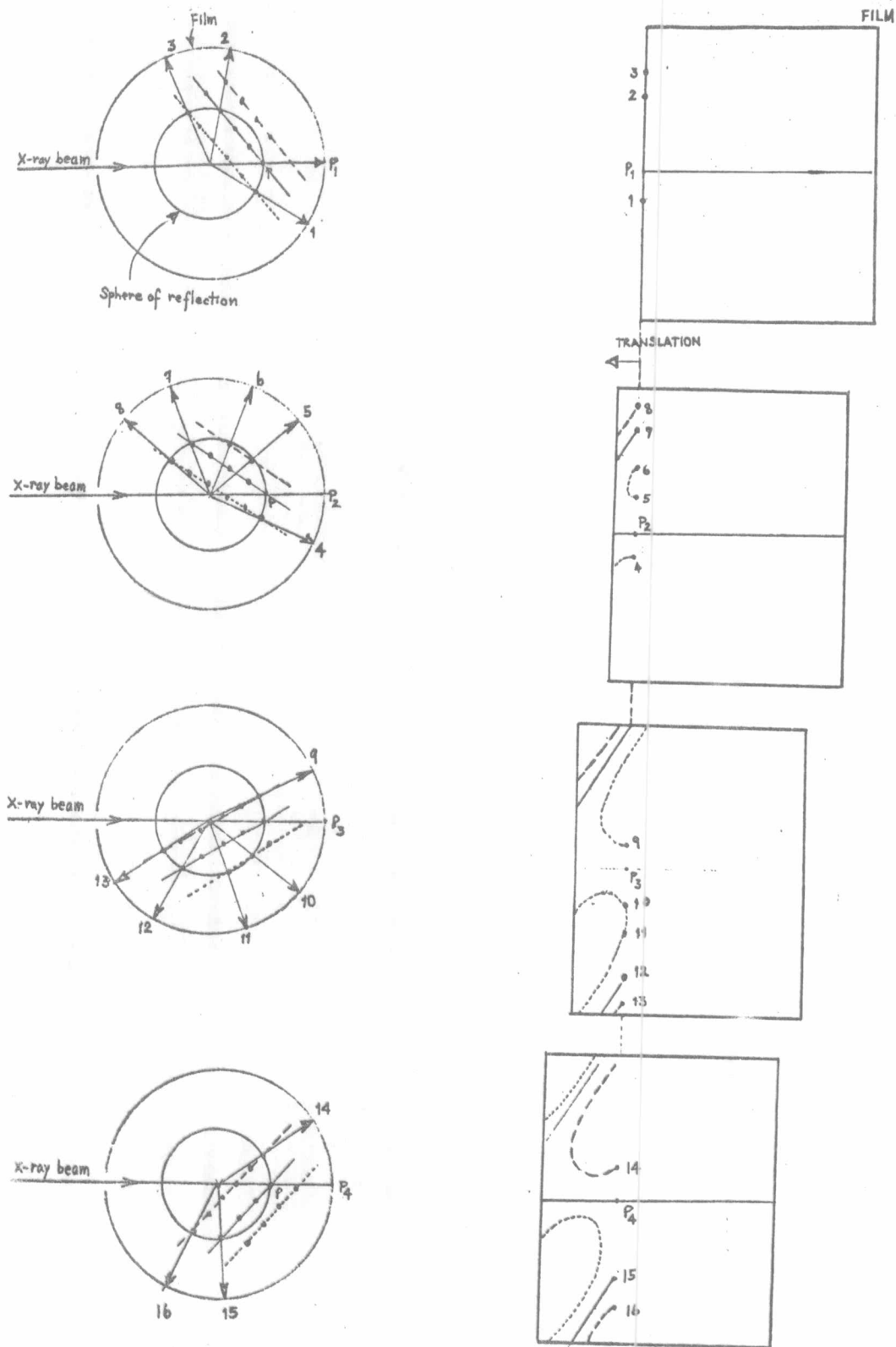and λ is the wavelength of the radiation.

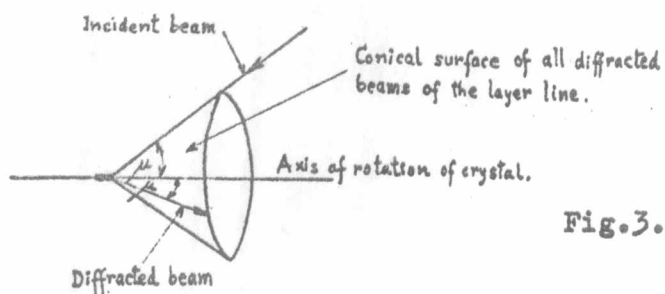Fig.3.1.8 Zero level, central and noncentral lines.

Fig.3.1.9 The equi-inclination
arrangement for non-zero
level Weissenberg photograph.

We get the Weissenberg photograph in form of the inter-
sections of sets of lines as in Fig.3.1.10. The lines are labelled
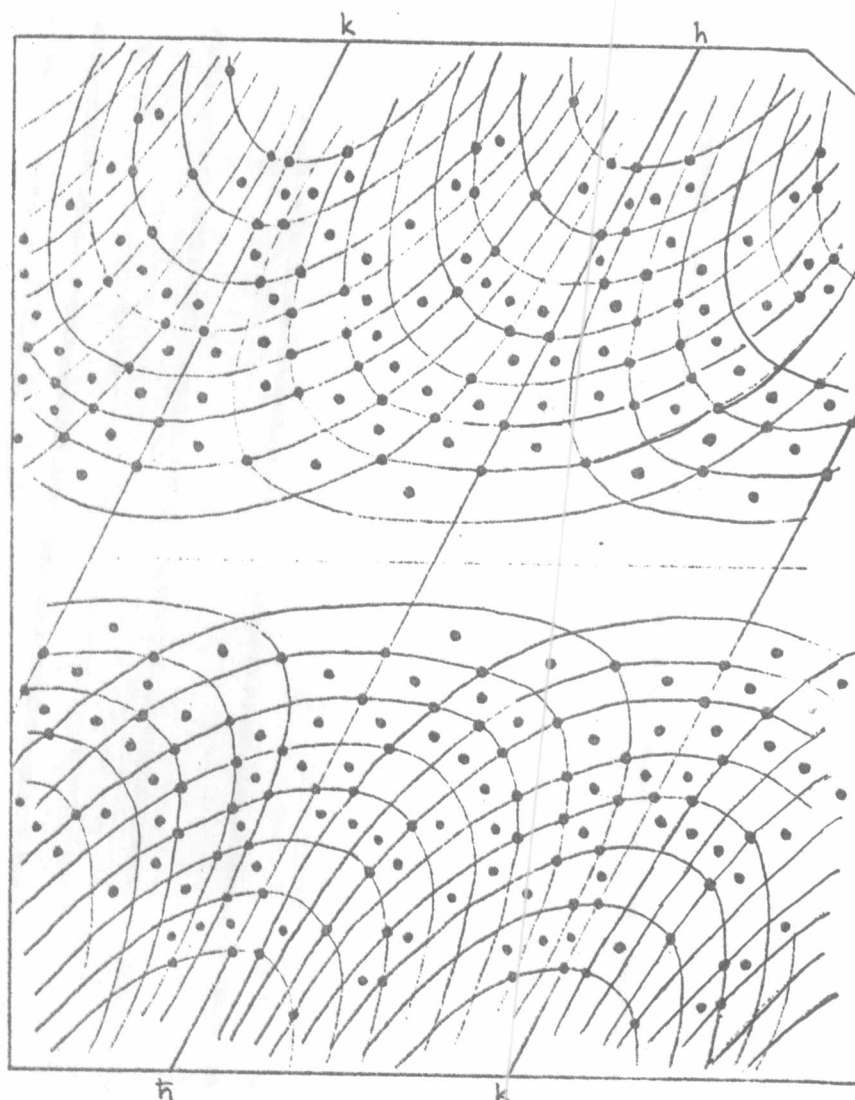with indices h and k when the rotation axis is c axis.

Fig.3.1.10 Weissenberg photograph.

3.2 Choosing crystals

Triniobium arsenide was obtained from the Institute of Chemistry, University of Uppsala, Uppsala, Sweden. These samples were prepared by heating the mixtures of Nb and NbAs in an argon-arc furnace.

A single crystal was picked out of the sample and its diffraction property was examined by using the oscillation and Weissenberg cameras with MoK_α radiation.

A suitable crystal for collecting X-ray diffraction data must be a single crystal. The external character of the crystal that was used was needle-like with regular sharp edges.

Crystals were examined from a microscope and the size of this crystal was measured under a calibrated microscope.

The trial-and-error method was used to determine whether the chosen crystal was a single crystal or not. It involved a search through a number of X-ray diffraction photographs of a number of crystals of Nb_3As.

3.3 Mounting and centering the crystal

The single crystal of Nb_3As was mounted on a fine glass fibre as shown in Fig.3.3.1.   Canada balsam was used to attach the crystal onto the fibre.   The end of the fibre was dipped into the Canada balsam and transferred quickly onto the crystal and adjusted so that a needle axis was parallel to the rotation axis.   The mounted crystal was then transferred to the goniometer head.
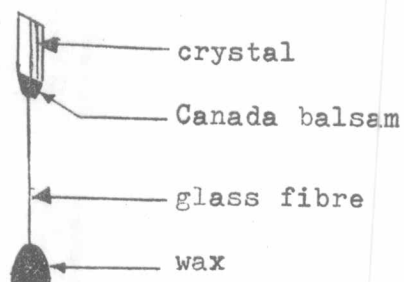

Fig.3.3.1 Mounted crystal.

The orientation of the crystal could be adjusted by two mutually perpendicular arcs of the goniometer as in Fig.3.1.2. The length of the glass fibre was such that the crystal would occupy the same position as the center of curvature of the arcs. A pair of arcs was attached to the spindle which were capable of angular adjustment over a limited range $\pm 20^{\circ}$, with vernier measurement to 0.1°.   The bottom arc had its axis perpendicular to the rotation axis.   The top arc was carried on the slide of the bottom arc.

The crystal may be roughly aligned by setting the arcs so that the assumed axis appeared parallel to the axis of rotation, but a more precise method was usually necessary as the crystal should be aligned to within at least 30' of arc.

The crystal was oriented on a rotation camera with the desired rotation axis direction in the equatorial plane, and perpendicular to the collimator axis. It must be moved by the linear arc slides so that its centre was not moved relative to the cross wire when the spindle was rotated. The height of the spindle was adjusted to bring the crystal into the centre of the beam.

The adjustment of the arcs could be calculated from measurements made on the oscillation film that the diffraction was in the form of layer lines. If no layer lines were visible, the axis of rotation was deduced as being so far from a crystal axis. This condition is shown by layer lines which are not straight or which are tilted with respect to the central axis of the oscillation photograph.

A setting photograph was taken with both arcs at zero. It was assumed that the upper arc U was parallel to the X-ray beam and the lower arc L was perpendicular to it as shown in Fig. 3.3.2.

Fig. 3.3.3 shows an error of setting in plane U of the upper arc, as the crystal was tipped toward the X-ray source which resulted in the tipping of the reciprocal lattice with respect to the X-ray beam. In general, the trace on the central

part of the film is caused by the X-ray beam which is diffracted by the crystal through the circle where the zero plane cut the sphere of reflection.
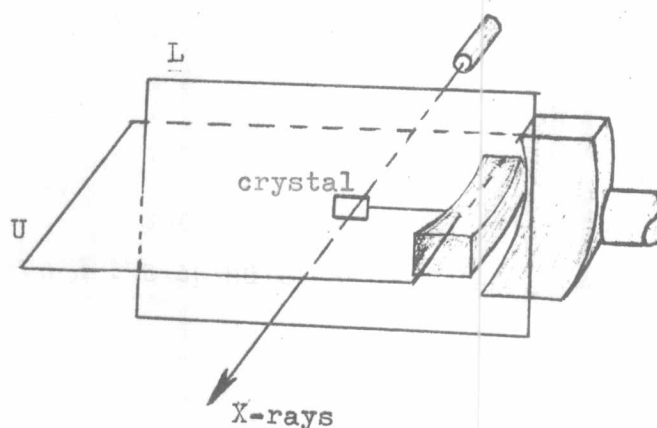

Fig.3.3.2 A goniometer head relative to two
perpendicular planes.

A curved layer line was called "bow".   If the crystal was rotated through 180°, a mirror-image pattern is formed as shown in Fig.3.3.3.

If the error was in plane L, the reciprocal lattice inclined at angle ε to the beam in a vertical plane.   The circle cut on the sphere of reflection which was rotating about the X-ray beam, however, it was not perpendicular to the axis of crystal rotation.   The trace was tilted with respect to the central axis of the film as shown in Fig.3.3.4.   The curve was called "tilt".   When the crystal was rotated through 180°, it formed the pattern of the mirror-image.
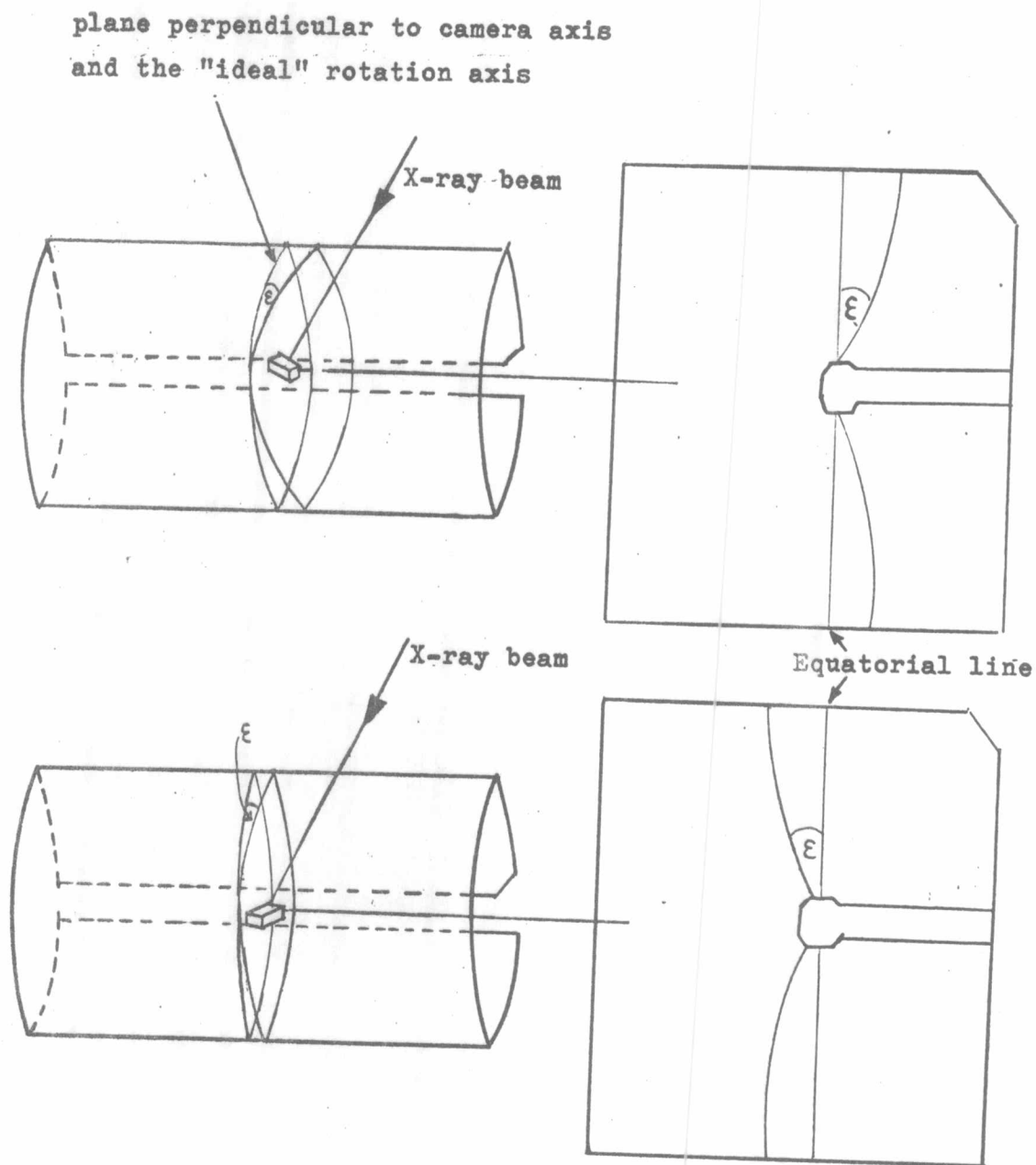
plane perpendicular to camera axis
and the "ideal" rotation axis

X-ray beam

ε

Equatorial line

X-ray beam

X-ray beam

ε

ε

ε

Fig. 3.3.3 Alignment error in plane U and zero

layer trace on film.

plane perpendicular to camera axis
and the "ideal" rotation axis

X-ray beam

ε

Equatorial line

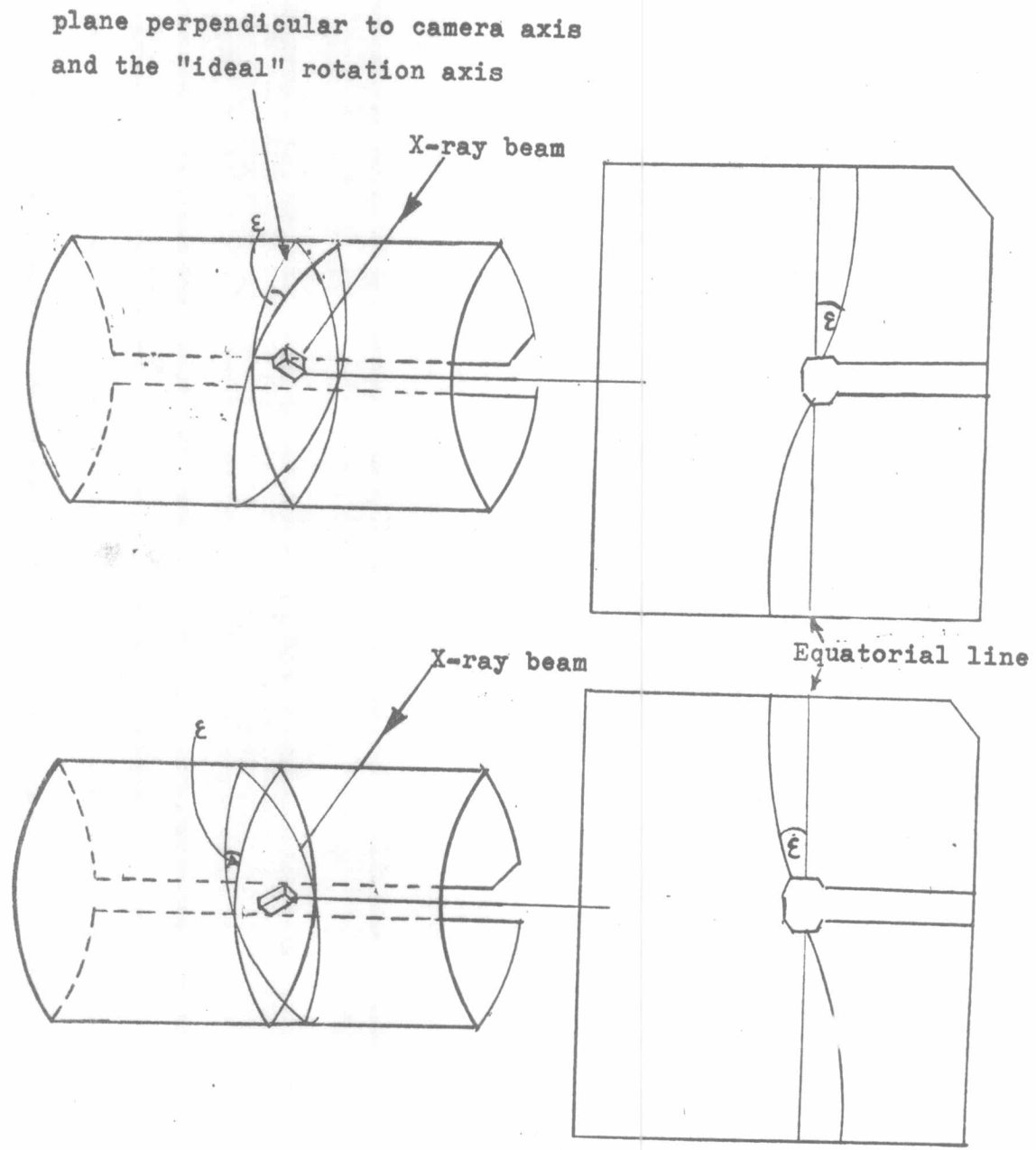X-ray beam

ε

Fig.3.3.4 Alignment error in plane L and zero
layers trace on film.

In Fig.3.3.5 was the 20° unfiltered oscillation photo-
graph with $\omega = 220^{\circ}$ at the mid-point of the oscillation so that
the scales of with the upper and lower arcs can be easily obser-
ved and they are approximately in the horizontal and vertical
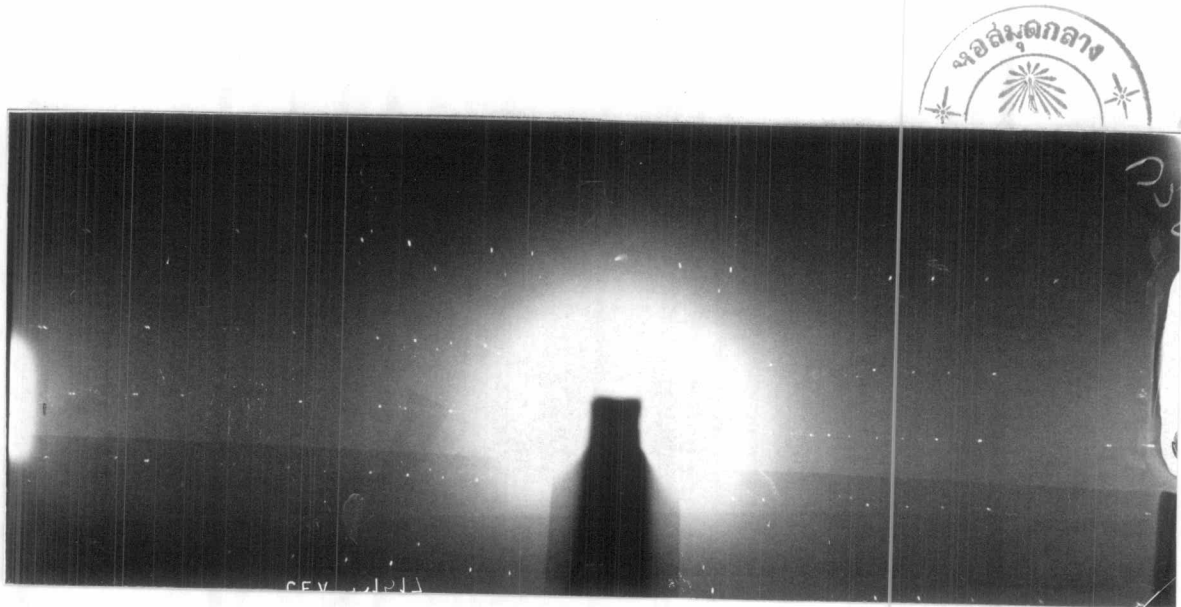planes respectively.

Fig.3.3.5 A setting photograph was taken with
both arcs at zero.

From this photograph, the zero layer trace is "tilt". The adjustment of orientation could be done by adjusting the lower arc axis.   It was corrected by measuring the value of angle ε as in Fig.3.3.4.   The fibre was brought upright by moving the lower arc ε^{o} in the anti-clockwise direction.

After correcting the orientation about the lower arc axis, a second oscillation photograph was taken at right angles to the first, mid-point at $\omega = 130^{o}$, and a correction made about the axis of the upper arc.

If it was certain that such a crystal was less than 5° mis-set, then it required a final setting.

The unfiltered oscillation photograph was taken with the upper arc perpendicular to the beam when the scale was towards the observer, at the ω scale reading 310°. Then the other photographs were taken in the same film at the ω scale reading 220°, 130° and 40° respectively as shown in Fig.3.3.6 bringing the arcs to be alternately in the vertical and horizontal planes.

The distance between the zero layer curves of the photograph in positions 1 and 3 at $\pm x$ from the origin could be measured. This was repeated for the two curves in positions 2 and 4.   We could get from the positions 1 and 3

$$\tan 2\alpha_1 \quad = \quad \frac{c-d}{2x}$$

hence

$$\alpha_1 \quad = \quad \frac{1}{2} \tan^{-1}\left(\frac{c-d}{2x}\right) \quad \cdots (3.3.1)$$

and from positions 2, 4,

$$\tan 2\alpha_2 = \frac{a - b}{2x}$$

$$\alpha_2 = \frac{1}{2}\tan^{-1}\left(\frac{a-b}{2x}\right) \cdots (3.3.2)$$
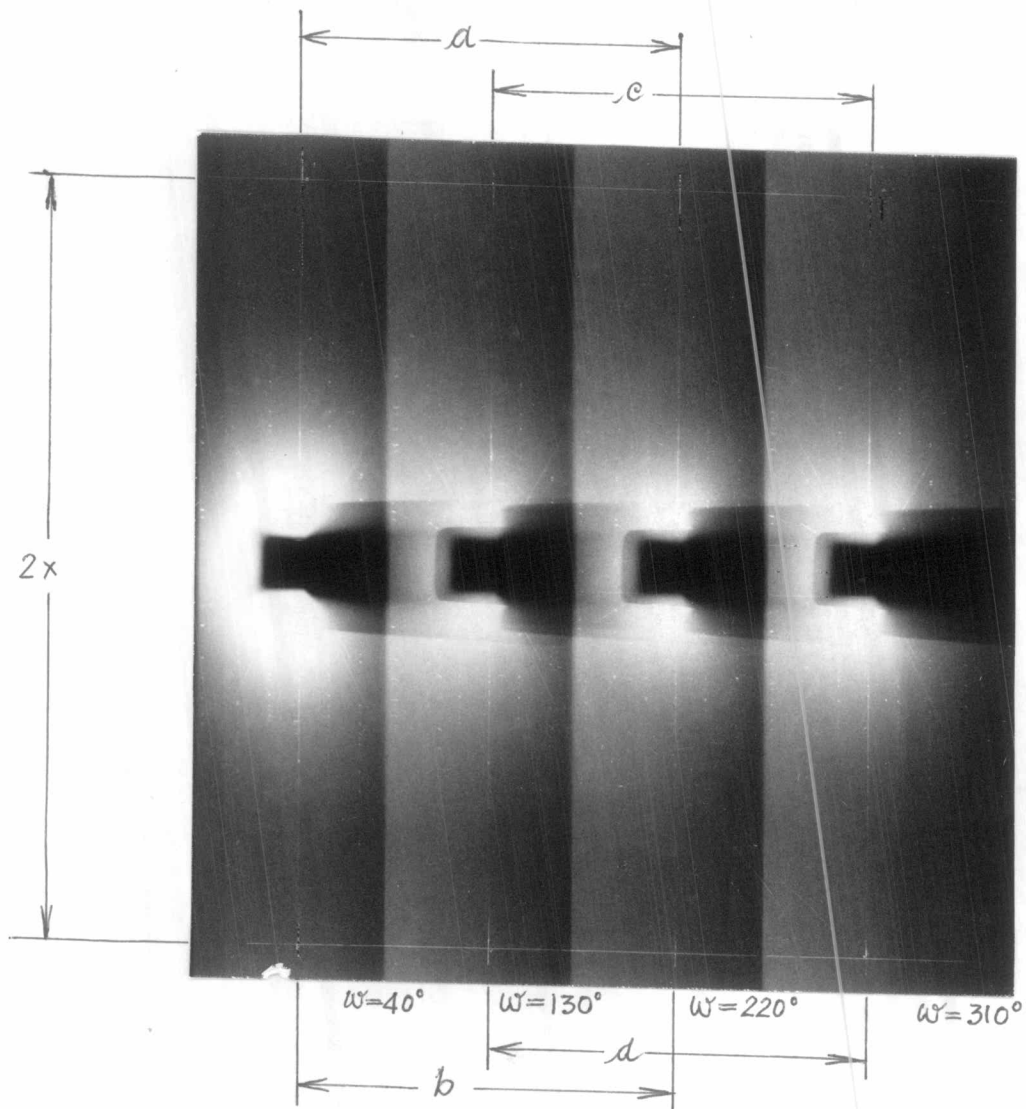

Fig.3.3.6 The final setting photograph.

where   a was the distance between the lines 2 and 4 at x,

               b was the distance between the lines 2 and 4 at -x,

               c was the distance between the lines 1 and 3 at x,

and   d was the distance between the lines 1 and 3 at -x.

A correction was then made by moving the axis of the upper arc α_1^0 and the axis of the lower arc α_2^0 .

This was repeated until the crystal was adjusted so that its main axes are exactly perpendicular to the rotation axis of the crystal ready for oscillation, rotation and Weissenberg photographs to be made.

3.4 Preliminary investigation of the structure of Nb_3As

3.4.1 Measurement of axial lengths and angles

The crystal was mounted with a selected axis of the direct c axis. An oscillation photograph was taken by using a long oscillation range $\omega = 0°$ to $200°$ about this axis during the exposure with MoK_α radiation and the filter Zr for 12 hours. This and subsequent photographs were to be taken by Mo radiation operating at 35 kv, 20 mA. on Philips, PW 1010/80.

In Fig.3.4.1, the oscillation photograph about the rotation axis c shows the layer lines which are related to levels in the reciprocal lattice.

From the equation (3.1.3) , c is the value of the rotation axis length , c axis , and r is the radius of the camera = 28.65 mm.

By measuring the distance between the pair of layer lines, the length of the c axis was calculated.

The results of measuring the film in Fig.3.4.1 were given in Table 3.4.1. From the calculation, the value of the c axis is 5.126 A° with a probable accuracy of 0.072 A°.

The value of the axis of Nb_3As could be obtained from remounting and rotating the crystal about the a axis.

The oscillation photograph was taken about the a axis at the range of 0° to 200°, exposed for 12 hours using MoK_α

radiation and the Zr filter. The photograph was shown in Fig. 3.4.2.

The value of the a axis was calculated from this photograph as shown in Table 3.4.2

Table 3.4.1 Measurement of an oscillation photograph.

Rotation Axis c.

MoK$_\alpha$ Radiation $\lambda_{K_\alpha} = \frac{1}{3}(2\lambda_{K_{\alpha_1}} + \lambda_{K_{\alpha_2}})$

$= \frac{1}{3}(2\times0.70926+0.71354)=0.71068\ A^\circ$

Camera Radius , R = 28.65 mm.

layer line	2Y (mm)	Y (mm)	$\frac{Y}{R}$ = tan ν	sin ν	$\frac{\lambda}{\sin\nu} = \frac{c}{n}$ (A°)	c (A°)
1	8.15	4.075	0.1422	0.1408	5.047	5.047
2	16.30	8.150	0.2845	0.2736	2.598	5.196
3	26.82	13.410	0.4681	0.4239	1.677	5.031
4	37.70	18.850	0.6579	0.5496	1.293	5.172
5	53.90	26.950	0.9407	0.6852	1.037	5.185

The value of the c axis of Nb_3As is $5.13 \pm 0.07\ A^\circ$

Table 3.4.2   Measurement of an oscillation photograph.

Rotation axis a

MoK$_\alpha$ radiation λ_{K_α} = 0.71068 Å.

Camera radius   R   =   28.65   mm.

layer line	2y (mm.)	y (mm.)	$\frac{y}{R}$ = tanν	sinν	$\frac{\lambda}{\sin\nu} = \frac{a}{n}$ (Å)	a(Å)
1	4.00	2.000	0.0698	0.0696	10.211	10.211
2	7.95	3.975	0.1387	0.1374	5.172	10.344
3	11.95	5.975	0.2086	0.2042	3.480	10.440
4	16.25	8.125	0.2836	0.2728	2.605	10.420
5	20.90	10.450	0.3648	0.3427	2.074	10.370
6	26.25	13.125	0.4581	0.4165	1.706	10.236
7	31.70	15.850	0.5532	0.4841	1.468	10.276

The value of the a axis of Nb_3As is 10.33 ± 0.09 Å.

Fig. 3.4.1   Oscillation photograph of Nb₃As rotated about
c axis MoK$_\alpha$ radiation, for 12 hours exposure.

Fig. 3.4.2   Oscillation photograph of Nb₃As rotated about
a axis MoK$_\alpha$ radiation, for 12 hours exposure.

The other two axes, other than the rotation axis, and the angles are obtained from various layers of Weissenberg photographs.

Two instrumental settings, namely the equi-inclination angle, μ, and the layer line screen setting, s, had to be determined for the upper level photographs.

The equi-inclination angle, μ. The inclination angle arrangement is the most useful of the Weissenberg methods, the relation

$$\mu = \sin^{-1}\left(\frac{n\zeta}{2}\right) \qquad \dots (3.4.1)$$

where $\zeta = \dfrac{\lambda}{c}$,

if c is the rotation axis that is obtained from the measurement from the oscillation photograph,

n is the number of layer lines,

and λ is the wavelength of the radiation.

The values of the equi-inclination angle for the various upper level photographs are shown in Table 3.4.3a. and b.

The layer line screen setting, S. The screen could be moved an appropriate distance of S mm. fro `ts zero-level position to permit the reflections from a particular upper level to reach the film are shown in Table 3.4.3a. and b.

The distance is relative to the radius of the layer-line screen R_S, and the inclination angle μ,

$$S = R_S \tan\mu \qquad \dots (3.4.2)$$

Table 3.4.3 The instrumental settings; inclination angle μ and

layer line screen S for various layers of Nb_3As.

a. Rotation axis, c = 5.13 ± 0.07 Å , $\zeta = \dfrac{\lambda}{c} = 0.14$

MoK_α radiation, $\lambda = 0.71068$ Å .

Camera radius , $R_S = 28.65$ mm.

layer line	$\dfrac{n\zeta}{2}$	$\mu=\sin^{-1}\left(\dfrac{n\zeta}{2}\right)$	tan μ (±0.04)	$S = R_S \tan\mu$ ±1 (mm.)
0	0	0	0	0
1	0.07	4.0	0.0695	2.01
2	0.14	8.1	0.1400	3.57
3	0.21	12.1	0.2125	5.42
4	0.28	16.1	0.2885	7.36

b. Rotation axis , a = 10.33 Å , $\zeta = \dfrac{\lambda}{a} = 0.07$

MoK_α radiation, $\lambda = 0.71068$ Å .

Camera radius , $R_S = 28.65$ mm.

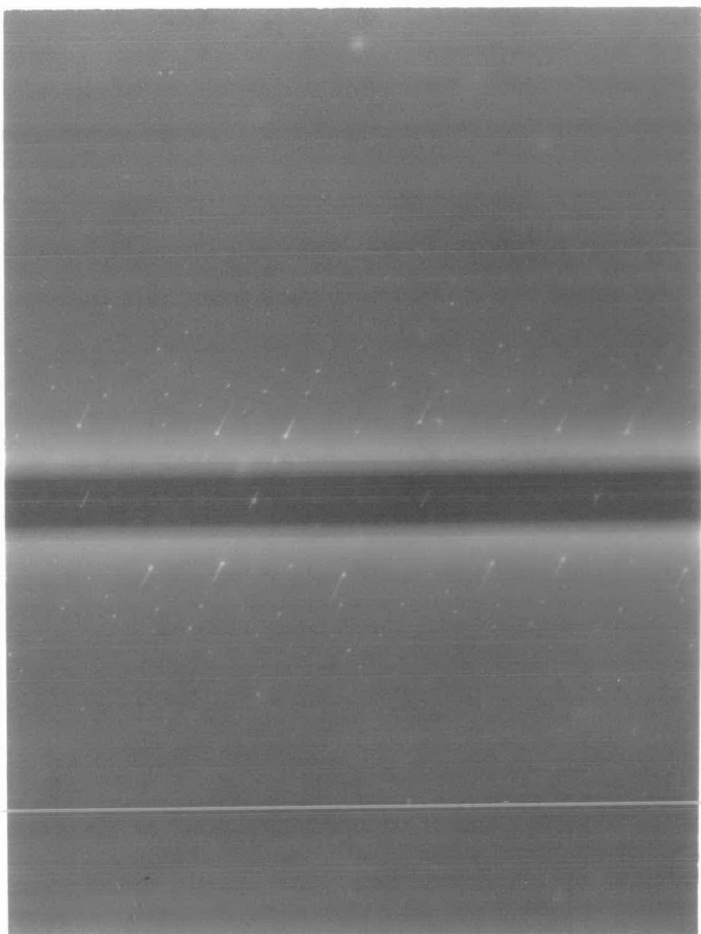| layer line	$\dfrac{n\zeta}{2}$	$\mu=\sin^{-1}\left(\dfrac{n\zeta}{2}\right)$	tan μ	$S = R_S \tan\mu$ (mm.)
0	0	0	0	0
1	0.04	2.3	0.0400	1.15
2	0.07	4.0	0.0699	2.00
3	0.11	6.3	0.1104	3.16
4	0.14	8.1	0.1423	4.08

Fig. 3.4.3   Weissenberg photograph 0th layer (hk0)

Fig. 3.4.4   Weissenberg photograph 0th layer (0kl)
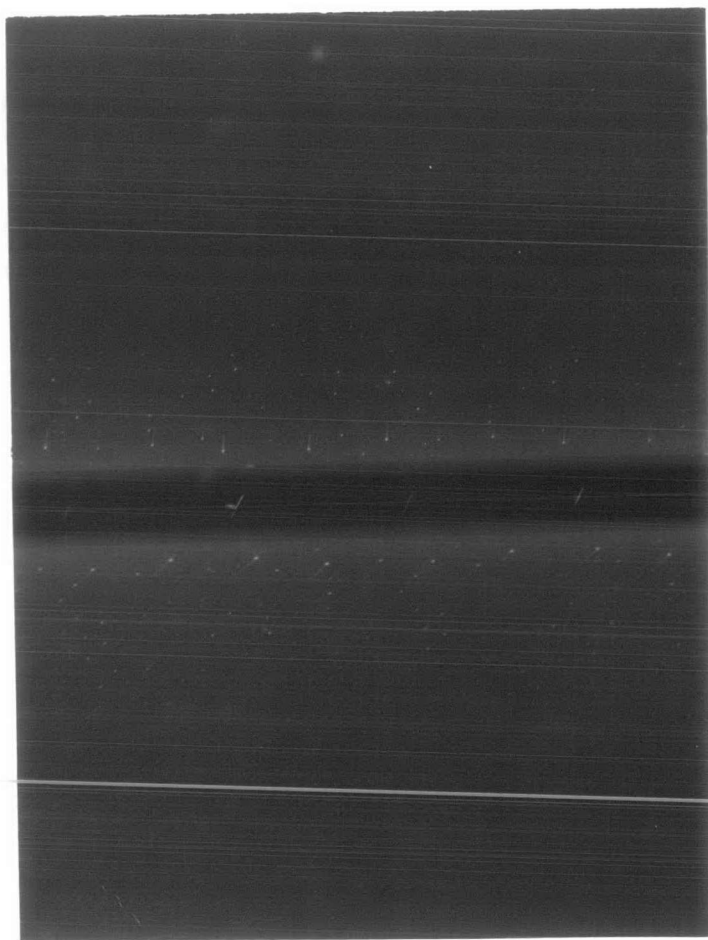
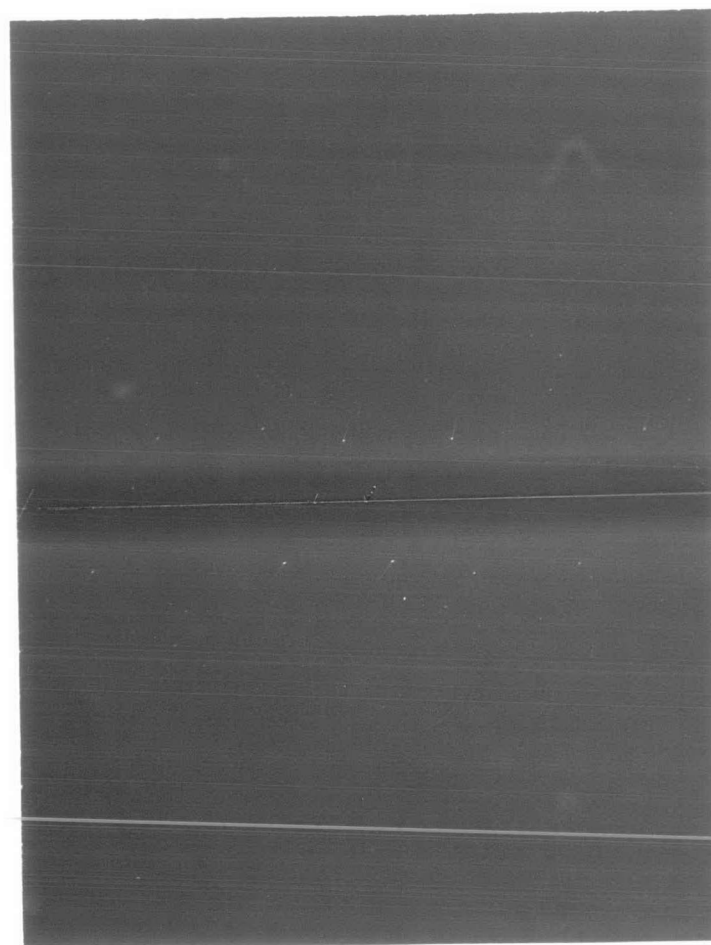Fig. 3.4.5   Weissenberg photograph 1st layer (hkl)

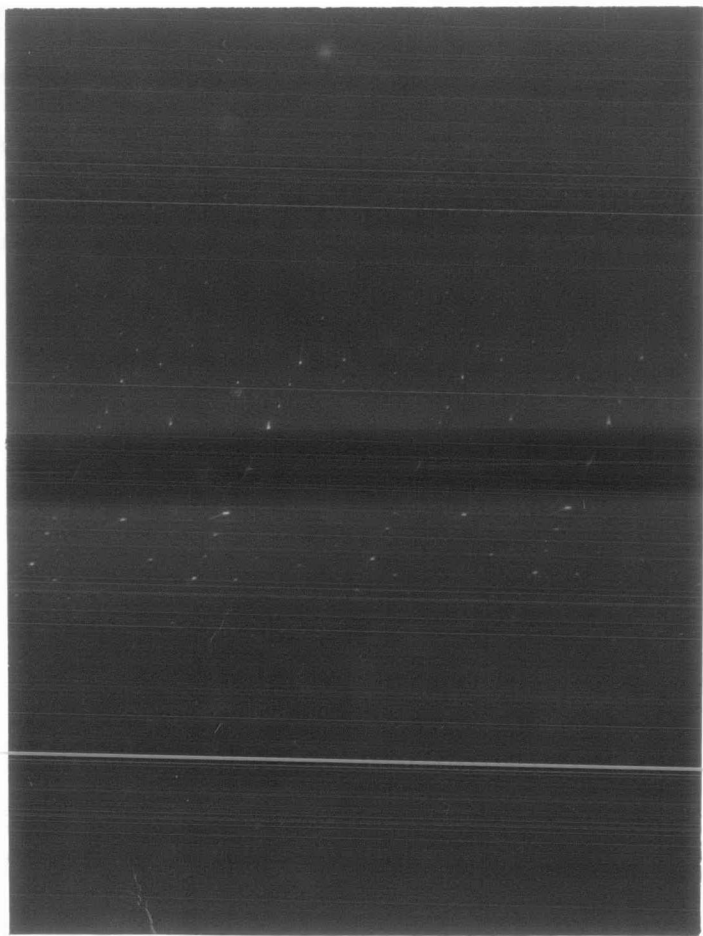Fig. 3.4.6   Weissenberg photograph 1st layer (lkl)
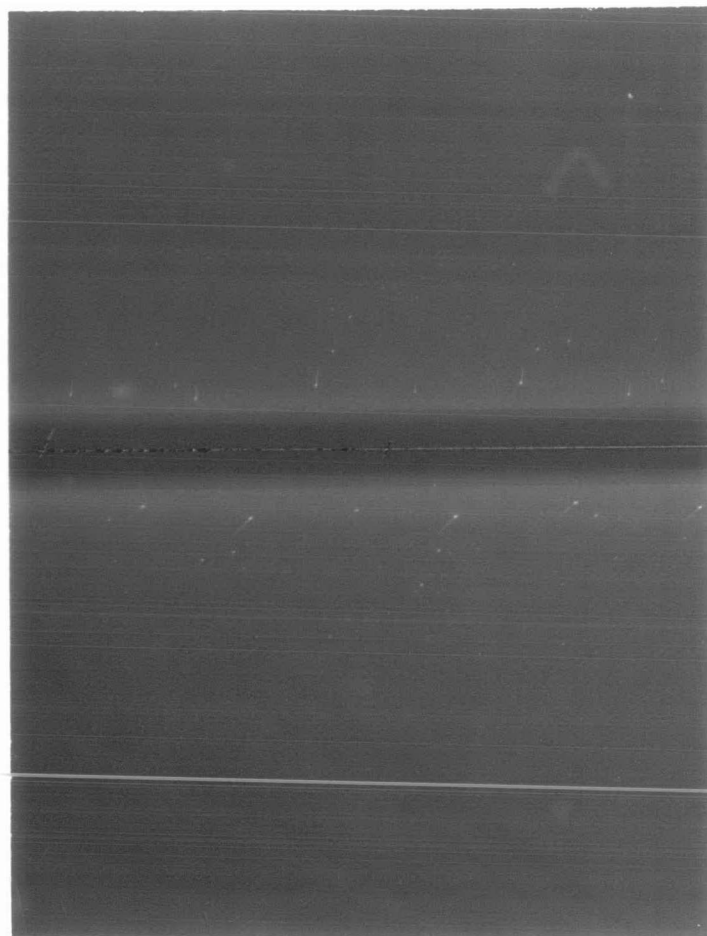
Fig. 3.4.7   Weissenberg photograph 2nd layer (hk2)

Fig. 3.4.8   Weissenberg photograph 2nd layer (2kl)

67

The Weissenberg photographs were taken on zero, first, and second layers, as in Fig.3.4.3, 3.4.5 and 3.4.7, using free translation of the film carriage of 110 mm., corresponding to an oscillation range of $0^{\circ} - 220^{\circ}$ about **c axis**.

The Weissenberg photographs were taken on **zero**, first, and second layers, as in Fig.3.4.4, 3.4.6 and 3.4.8, using the oscillation range of $0^{\circ} - 220^{\circ}$ about a axis.

Each Weissenberg photograph uses the exposure time of 40 hours, with MoK_{α} radiation and the Zr filter.

The x and z coordinates of the reflections in these photographs corresponded to the ξ and Φ coordinate of the reciprocal lattice points as shown in Fig.3.4.9 are measured.
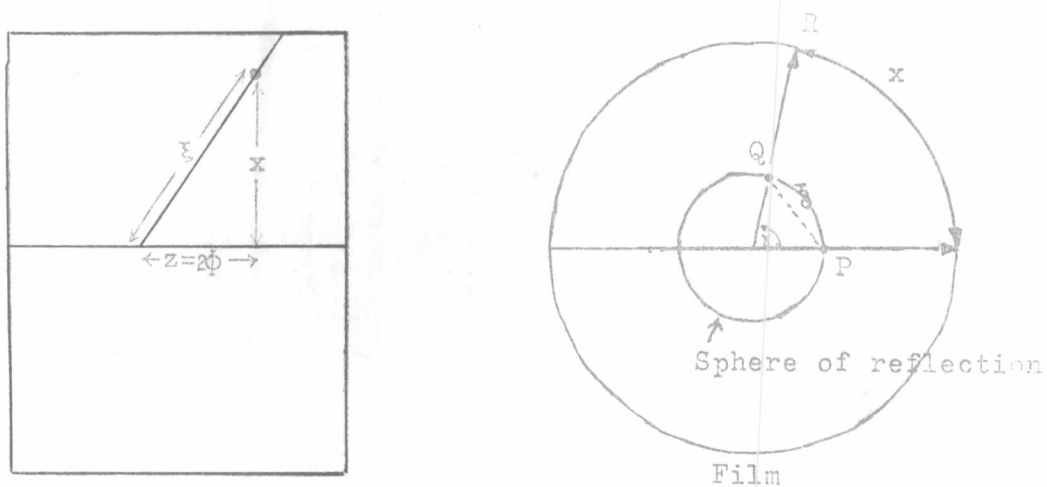
Fig.3.4.9 Cylindrical coordinate relative to film and reflection.

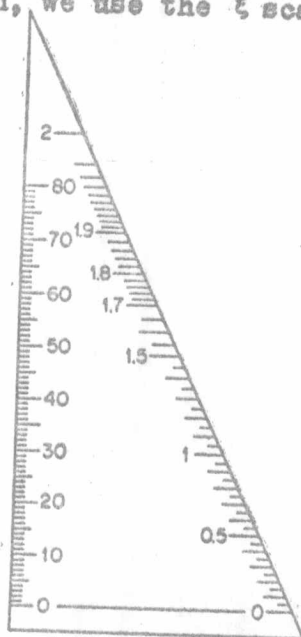To measure the ξ coordinate in the Weissenberg photograph, we use the ξ scale that is shown in Fig.3.4.10.

Fig.3.4.10 ξ scale .

The ξ scale rides on top of the centimeter scale that coincides with the position of zero ξ on the film. The value of ξ coordinate was measured in the reciprocal lattice unit (r.l.u.).

Because the axis passes through the origin, the ξ co-ordinate of points on axial rows, which lie in the zero layer, are indentical with the corresponding axial periods with the relation

$$a^* = \frac{\xi_{h00}}{h}$$

$$b^* = \frac{\xi_{0k0}}{k}$$

$$c^* = \frac{\xi_{001}}{l}$$

... (3.4.3)

where ξ refers to co-ordinates in the zero level.

a^*, b^* and c^* are the reciprocal axes.

By measuring the distance between the two points at which the projections cross the center line of the film , the

angle Φ between two central lattice rows that is related to the horizontal film distance z is determined by the relation

$$1 \text{ x z mm.} = 2 \text{ x } \Phi \text{ degrees} \quad \ldots \text{ (3.4.4)}$$

when the translation / rotation constant of the instrument is 1 mm./2°.

From the zero-level film in Fig.3.4.3 , the length of a and b axes and the angle γ^* are determined as shown in the Table 3.4.4.

From Fig.3.4.4 , the length of b and c axes and the angle α^* are determined as shown in the Table 3.4.5.

From Fig.3.4.3, the distance z between the two central lattice rows is 4 5 mm., it shows that the interaxial angle γ^* is 90° by the equation (3.4.4).

From Fig.3.4.4, the distance z is 45 mm. between the two central lattice rows, the interaxial angle α^* is 90° and α is therefore 90°.

Table 3.4.4   Measurement of a   zero layer Weissenberg photograph,
rotation axis c,

MoK$_\alpha$ radiation $\lambda = 0.71068 \text{ Å}$

a). a axis

hkl	ξ (r.l.u.)	$a^* = \dfrac{\xi_{h00}}{h}$	$a = \dfrac{\lambda}{a^*}$ (Å)
400	0.27	0.068	10.45
600	0.41	0.068	10.45

Table 3.4.4

(continued)

hkl	$\xi(r.l.u.)$	$a^* = \dfrac{\xi_{h00}}{h}$	$a = \dfrac{\lambda}{a^*}$ (Å)
800	0.54	0.068	10.45
1000	0.68	0.068	10.45
1400	0.94	0.067	10.61
1600	1.07	0.067	10.61

The value of the a axis of Nb_3As is 10.52 ± 0.08 Å.

b). b axis

hkl	$\xi(r.l.u.)$	$b^* = \dfrac{\xi_{0k0}}{k}$	$b = \dfrac{\lambda}{b^*}$ (Å)
040	0.27	0.068	10.45
060	0.41	0.068	10.45
080	0.54	0.068	10.45
0100	0.68	0.068	10.45
0140	0.94	0.067	10.61
0160	1.07	0.067	10.61

The value of the b axis of Nb_3As is 10.52 ± 0.08 Å.

Table 3.4.5 Measurement of a zero layer Weissenberg photograph,

rotation axis a,

MoK$_\alpha$ radiation , λ = 0.71068 $\overset{\circ}{A}$.

a). b axis.

hkl	ξ (r.l.u.)	$b^* = \dfrac{\xi_{0k0}}{k}$	$b = \dfrac{\lambda}{b^*}$ ($\overset{\circ}{A}$)
0100	0.69	0.069	10.30

b). c axis.

hkl	ξ(r.l.u.)	$c^* = \dfrac{\xi_{001}}{l}$	$c = \dfrac{\lambda}{c^*}$ ($\overset{\circ}{A}$)
004	0.55	0.138	5.15

3.4.2 Determination of the symmetry and the space group

From the oscillation photographs, certain basic symmetry elements are known; and more symmetry information can be obtained from Weissenberg photographs.

The oscillation photographs in Fig.3.4.1 and Fig. 3.4.2 show the presence of a mirror plane.   In the Weissenberg photographs, the intensities on the negative part of any noncentral lattice line are mirrored by those on the positive part. When the rotation axis is c , the a^* and b^* axes appear in the zero-level Weissenberg photograph.   The c^* axis of Nb_3As is

a four-fold axis in the reciprocal lattice.

The symmetry is also shown in the Laue photographs. The Laue photographs were taken along the a^* axis and c^* axis , during the exposure with MoK_α radiation, no filter, for 1 hour and they were shown in Fig.3.4.11 and Fig.3.4.12.

From the zero layer of the Weissenberg photograph we plotted a graph of the reciprocal lattice points of the present reflections that can be indexed, shown in Fig.3.4.13. This graph showed that the lattice of Nb_3As has a 4-fold axis and these symmetry elements belong to a tetragonal unit cell.

The space group of this crystal was determined from the systematic absences found in the Weissenberg photograph. Using the cylindrical co-ordinates, ξ and Φ of Weissenberg photographs from various levels to plot graphs between the two indices. When c is the rotation axis, the graphs of (hk0), (hk1), (hk2) and (hk3) are obtained. When a is the rotation axis, we can get (0kl), (1kl), (2kl) and (3kl). These graphs are shown in Fig.3.4.14.

From the graphs in Fig.3.4.14, the conditions of the possible reflections were found to be in Table 3.4.6.

Table 3.4.6 The condition of the possible reflections in the
(hk0) and (0kl) reflection data of Nb_3As

Class of reflection	Condition for reflections	Possible symmetry element
hkl	No systematic absences	P

Table 3.4.6

(continued)

Class of reflection	Condition for reflections	Possible symmetry element
hk0	$h + k = 2n$	$n \perp c$
001	$l = 2n$	4_2 along c
0k0	$k = 2n$	4_2 along b

These conditions agreed with the unique space group $P4_2/n$ in tetragonal system from the International Table Vol. I. Therefore Nb_3As is in tetragonal system , the point group is $4/m$ and the space group is $P4_2/n$.
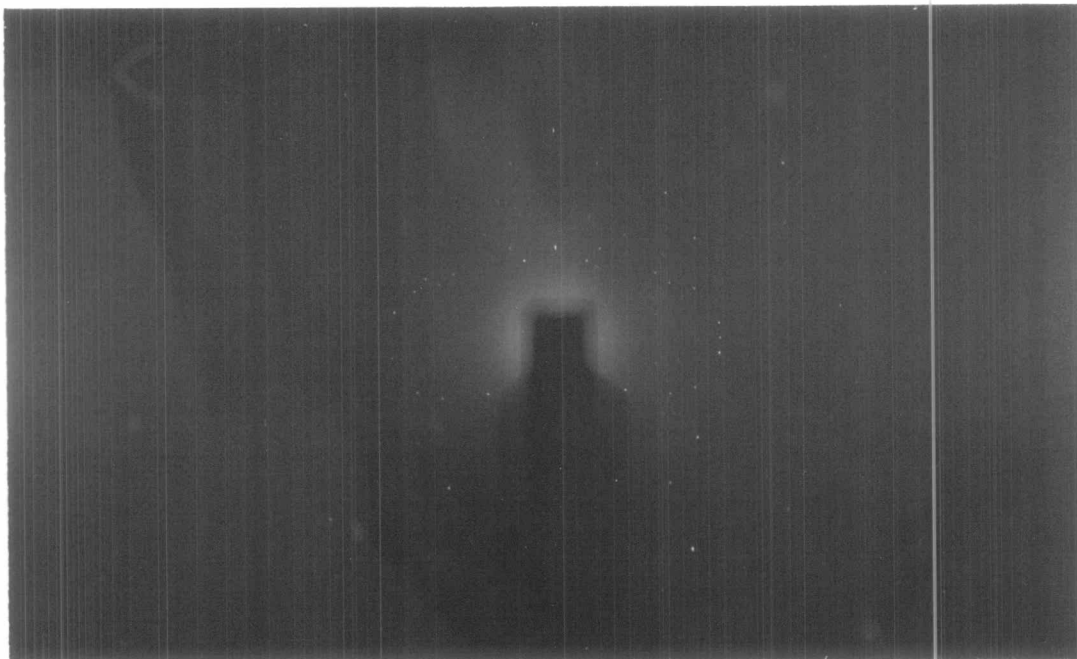
Fig. 3.4.11   Laue photograph taken along a axis

(perpendicular to c axis)
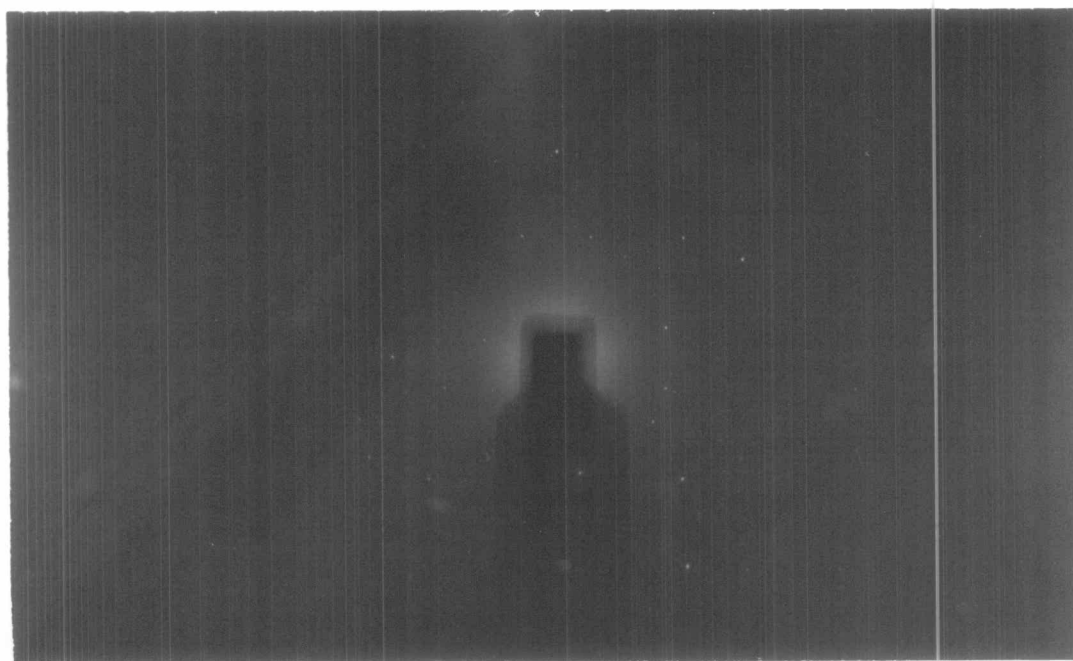
Fig. 3.4.12   Laue photograph taken along c axis

(perpendicular to a axis)
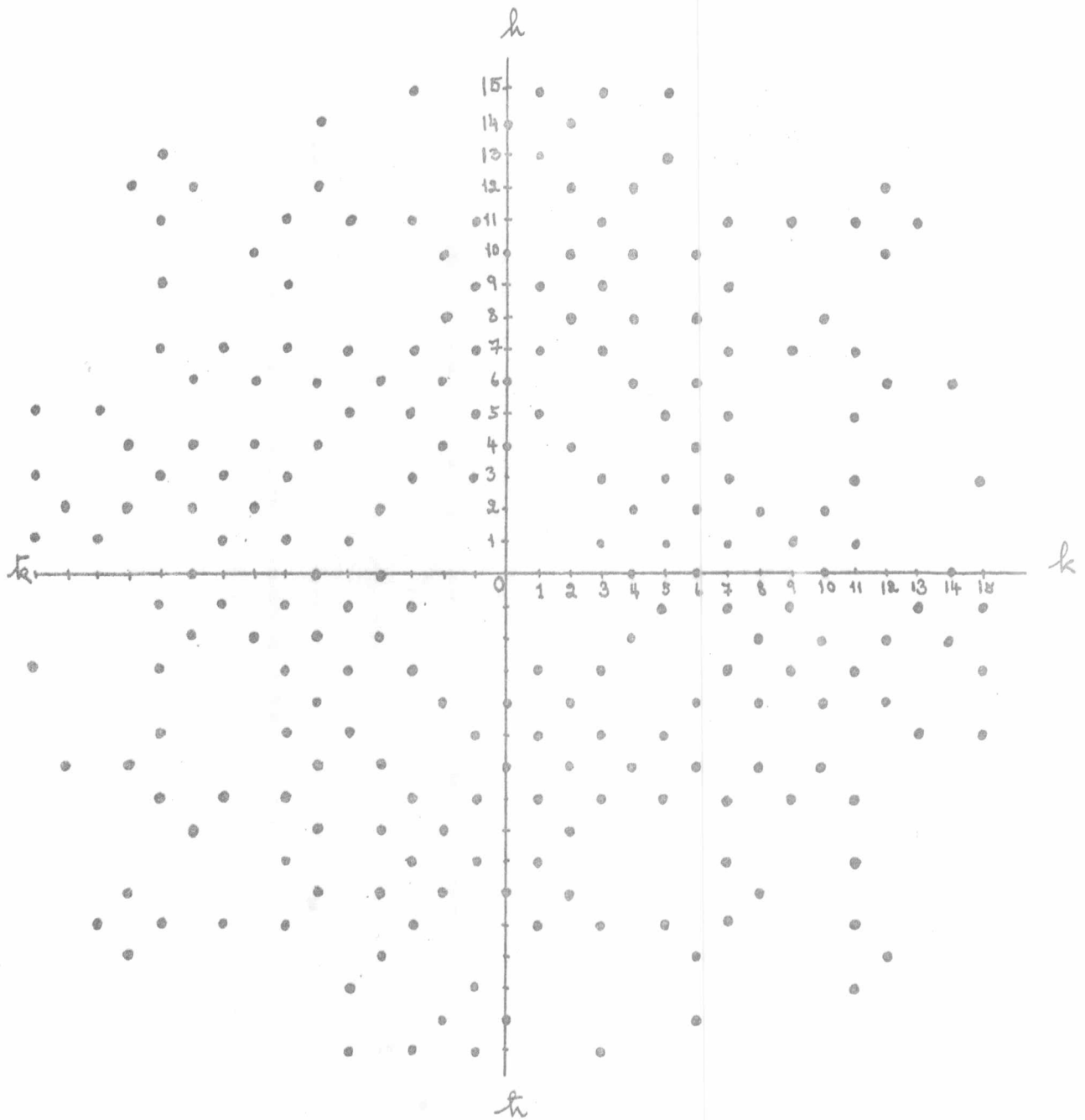
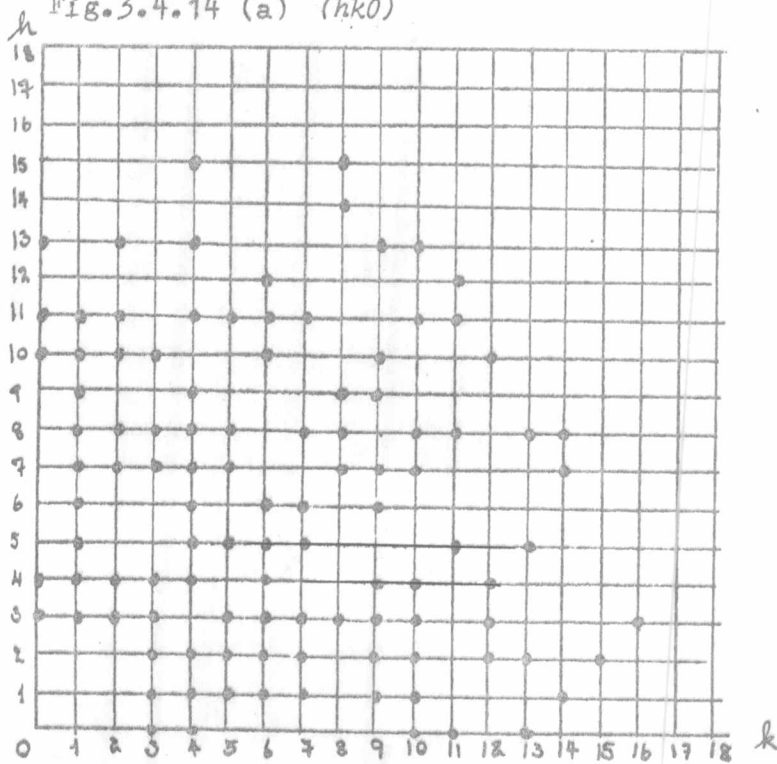Fig. 3.4.13 The hk0 reciprocal lattice.
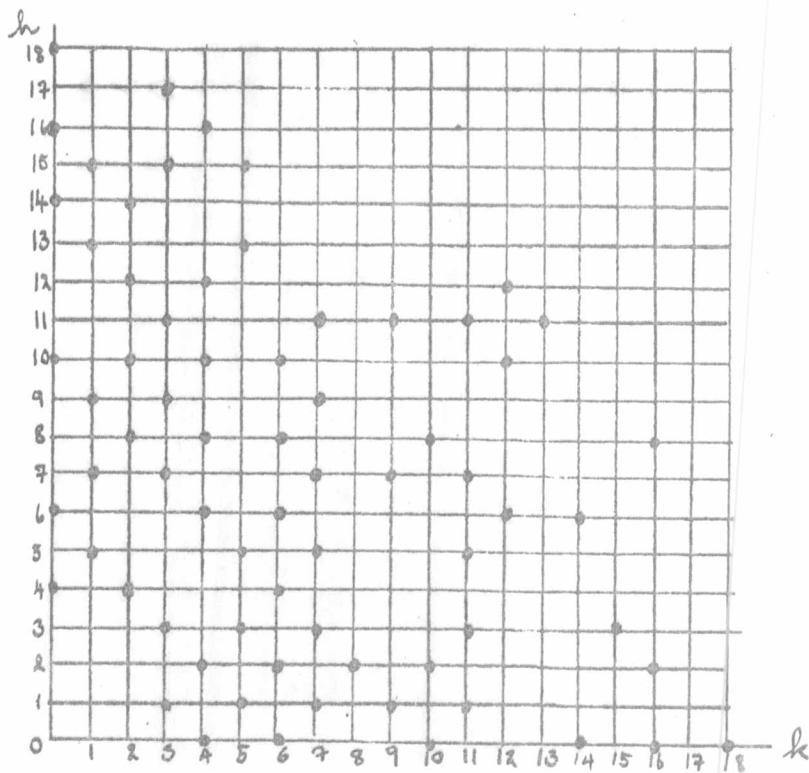
Fig.3.4.14 (a) (hk0)

Fig.3.4.14 (b)   (hk1)
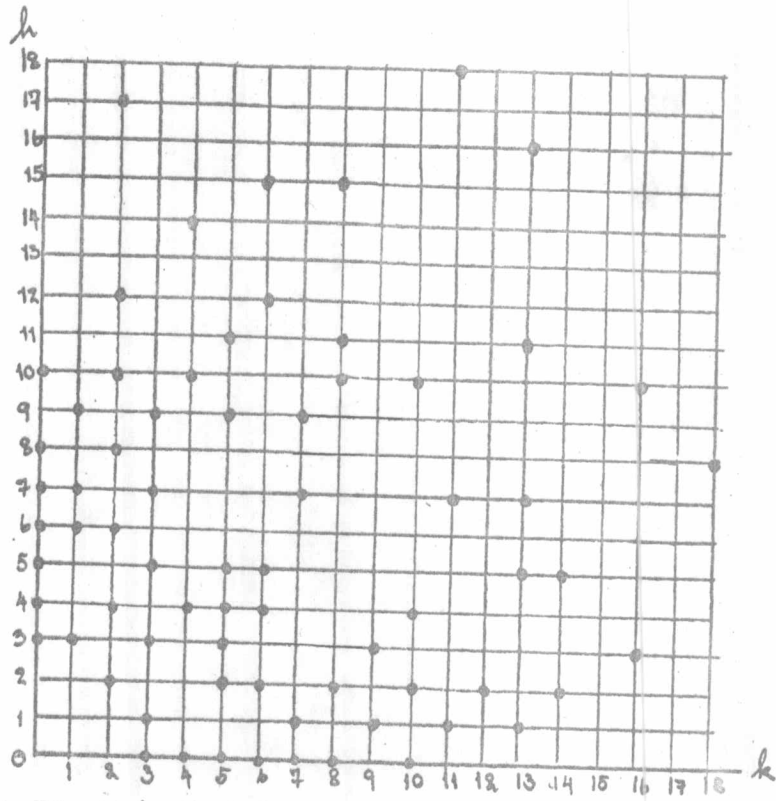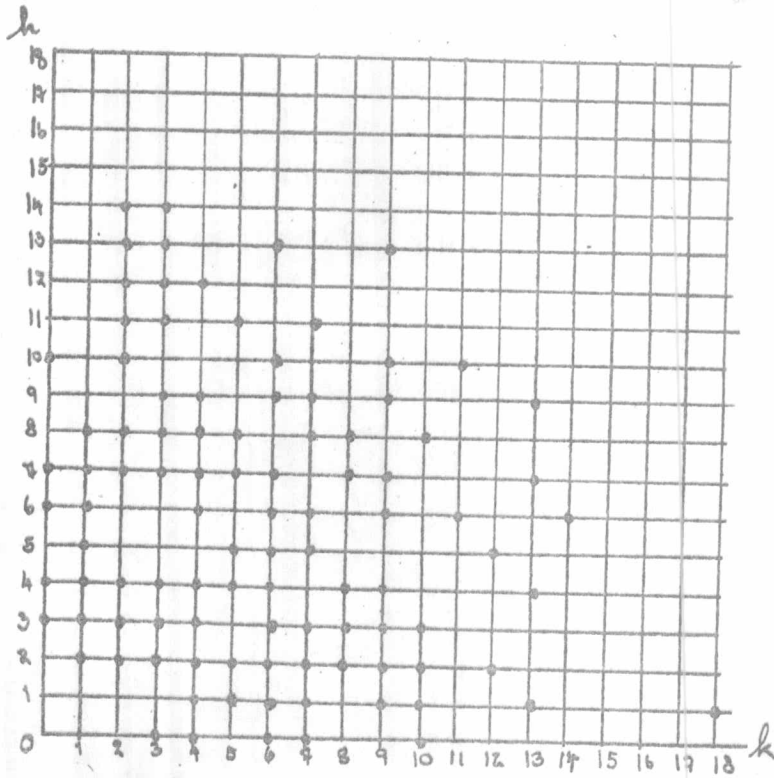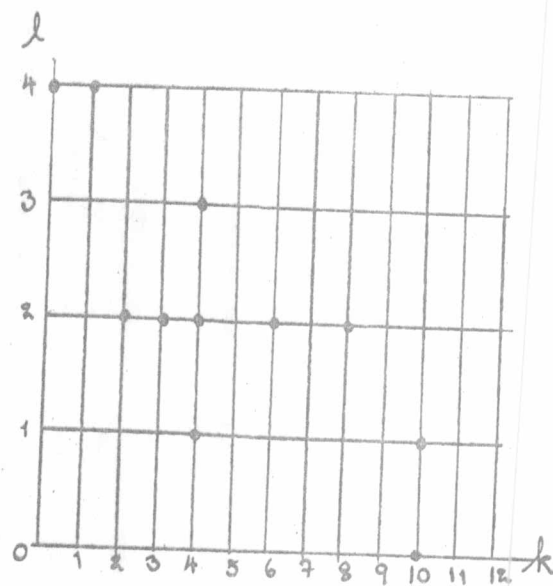
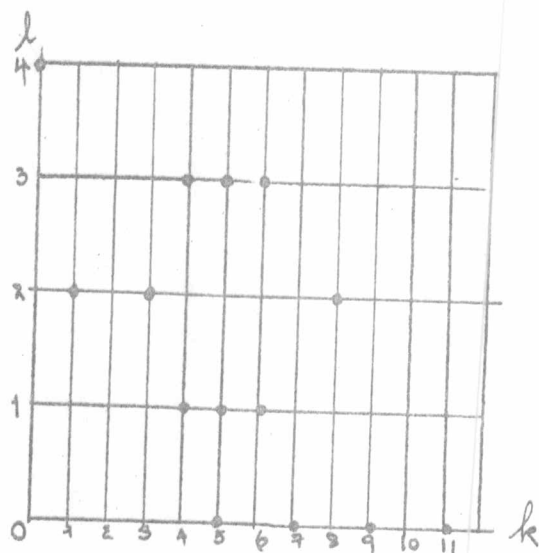Fig.3.4.14 (c) (hk2)

Fig.3.4.14 (d) (hk3)

Fig.3.4.14 (e)   (0k*l*)

Fig.3.4.14 (f)   (1k*l*)
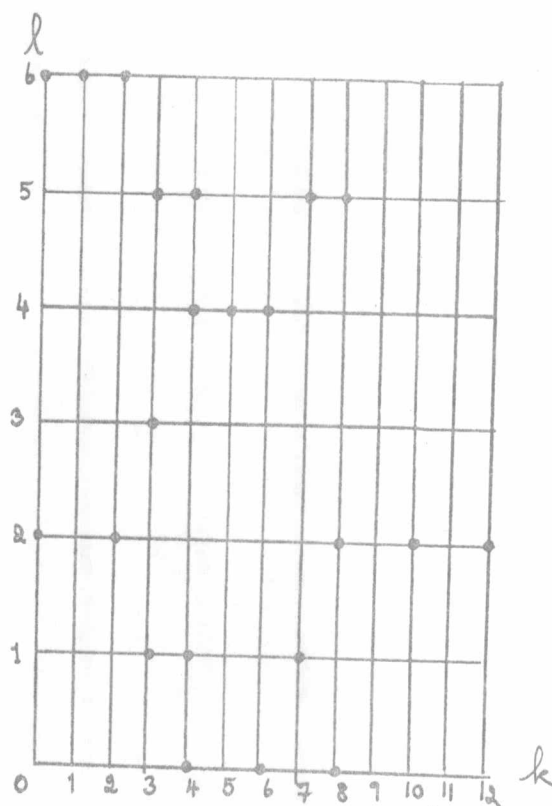
Fig.3.4.14 (g) (2kl)

Fig.3.4.14 A quadrant of reciprocal lattice as plotted
from (hk0), (hk1), (hk2), (hk3), (0kl), (1kl),
(2kl), and (3kl) Weissenberg photographs.

3.4.3 Calculation of the unit cell contents

The density of Nb_3As was determined and combined with the measured dimensions of the unit cell to give an accurate value for the total molecular weight of its contents and the number of molecules in the cell could be deduced.

The density of Nb_3As was experimentally found to be 7.9 ± 0.6 gm/c.c.

The volume of the unit cell of Nb_3As whose axes were deduced from section 3.4.4 is

$$V = abc$$
$$= 10.52 \times 10.52 \times 5.13 \quad \overset{\circ}{A}^3$$
$$= 567.27 \quad \overset{\circ}{A}^3$$

The unit-cell of Nb_3As weighs,

$$W = (567.27 \times 10^{-24}) \text{ cm.}^3 \times 7.9 \text{ gm/c.c.}$$
$$= 4.49 \times 10^{-21} \text{ gm.}$$

The weight of one molecule of Nb_3As is $(1.66 \times 10^{-24}) \times \{(93 \times 3) + 75\}$

$$= 1.66 \times 10^{-24} \times 3\ 54 \text{ gm/molecule.}$$

If the unit-cell of Nb_3As contains Z molecules, thus

$$Z = \frac{4.49 \times 10^{-21}}{354 \times 1.66 \times 10^{-24}}$$
$$= 7.6 \sim 8$$

A unit-cell of Nb_3As therefore contains 8 molecules. Then the calculated density of Nb_3As is $\dfrac{8 \times 354 \times 1.66 \times 10^{-24}}{567.27 \times 10^{-24}}$

$$= 8.29 \text{ gm/c.c.}$$

3.4.4 The absorption coefficient calculation

The computation of the linear absorption coefficient of Nb_3As was shown in Table 3.4.7.   The linear absorption coefficient could be computed from a knowledge of its chemical composition, its density, and a table of mass absorption coefficients of the elements, $\frac{\mu}{\rho}$, given in the International tables for X-ray Crystallography , Vol. III.

Table 3.4.7 The linear absorption coefficient for MoK_α

radiation of Nb_3As , density(ρ) = 8.29 gm/c.c.

Atom	Atomic weight	Total weight of atom in Nb_3As	Fraction of total wt.p(%)	$\frac{\mu}{\rho}$ (gm^{-1})	$p\left(\frac{\mu}{\rho}\right)$ (gm^{-1})
3Nb	93	279	78.81	17.1	13.48
As	75	75	21.19	69.7	14.77

$\Sigma p\left(\frac{\mu}{\rho}\right)$ for Nb_3As is 28.25 gm^{-1}

The linear absorption coefficient, μ , is μ = Density $\times \Sigma\, p\left(\frac{\mu}{\rho}\right)$

= 8.29 x 28.25 cm^{-1}

= 233.96 cm^{-1}

So Nb_3As has $\mu \sim$ 234 cm^{-1} for MoK_α radiation.

Using the value of μ and the size of the crystal, the absorption correction A^* for various Bragg's angle θ was extrapolated from International Table for X-ray Crystallography, Vol. III.   The crystal was assumed to be in a cylindrical form,

and its radius was measured by a microscope to be 1.442×10^{-3} cm.
The value of A^* as a function of θ and μr was tabulated, i.e.

μ (cm^{-1})	r (cm)	μr	A^* at various θ				
			$0°$	$22.5°$	$45°$	$67.5°$	$90°$
234	1.442×10^{-3}	0.34	1.83	1.76	1.73	1.69	1.68

3.5 Collecting intensity data

The multiple-film method was employed in the preparation of the Weissenberg photographs for the subsequent intensity measurement.   Different exposure times were used.   In order to reduce the number of exposures needed, three films were used in the camera for each exposure.   The film closest to the crystal removes a fraction of the X-radiation, acting as a filter before the second, which in turn reduces the intensity reaching the third.   Between each pair of films a sheet of developed film previously exposed to light was interleaved as a very thin Ag foil filter sheet.

The film factors will vary with the geometry of the camera used, they are determined for each set of photographs by calculating the intensity ratio for a number of pairs of reflections.   The films provide filter factor of 1.5 to 2 for MoK_α radiation.

The exposure times for each set of the hk0, hk1, hk2 Weissenberg photographs were 200, 43 and 10 hours, whereas the hk3, hk4 sets were recorded for 118 and 23 hours. The timing for the exposure was so that the intensity reduction ratio between successive films would be approximately constant at 1.7. The first photographs of 200 hours and 118 hours exposure of these layers were shown in Fig.3.5.1, 3.5.2, 3.5.3, 3.5.4 and 3.5.5.

The method of measurement involves the systematic comparison of the observed reflections against a calibrated density scale. This spot scale was prepared from an intense reflection from the crystal under studied of Nb_3As. It was prepared by

selecting an intense reflection for Nb_3As and taking repeated photographs of it by the Weissenberg method, at exposure times which were in the ratios desired for the final density scale. The film was shifted between each exposure so that the " new " reflection would not overlap onto the background of the foregoing reflection.

To make the measurements, the film was placed on a light box and the intensity of the reflection was compared with those of reference spots until a good match was found. Then the appropriate value was assigned as the observed intensity.

At the higher values of $\sin\theta$, the separation of K_{α_1} and K_{α_2} reflection becomes wider. The concerned spots were measured by combining the individual intensities of the separated spots of the same reflection, thus integrated intensities were measured.

When all the intensities had been measured, those from the second and latter films were multiplied by the corresponding filter factors for each of the preceding films, then the results were obtained on the same scale as the intensities measured on the first film.

The unmeasurable weak reflections are called unobserved reflections, the absence of reflections in the film is also an unobserved reflection. The intensity of the unobserved intensity is assigned to be less than the weakest observable reflection ($I_{min.}$), the value is $\frac{1}{2} I_{min.}$.
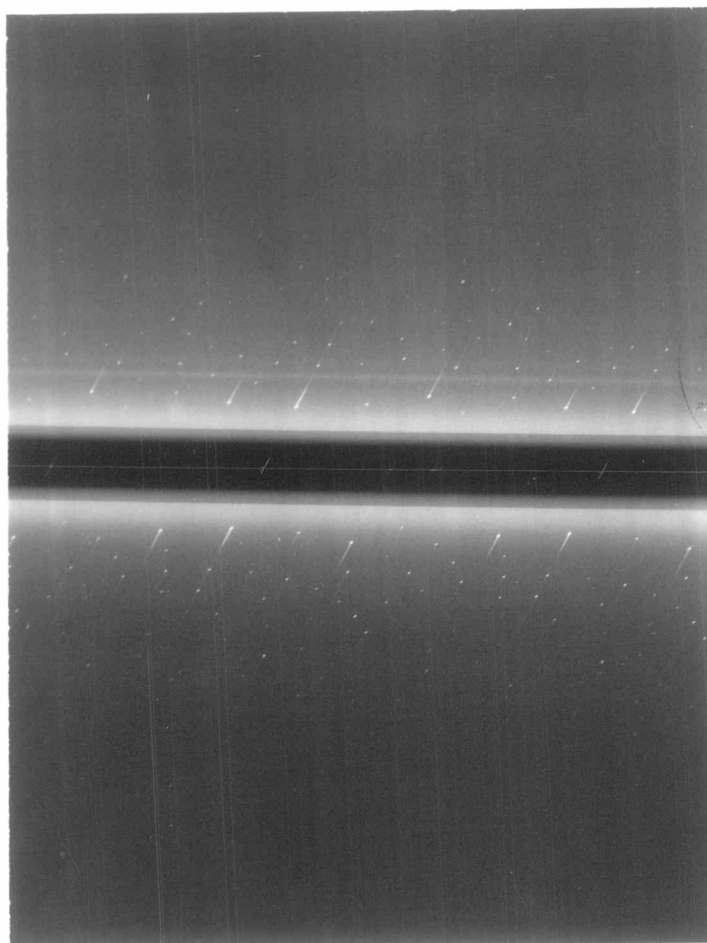
Intensity data Weissenberg photograph.

Fig. 3.5.1   Weissenberg photograph 0th layer (hk0)
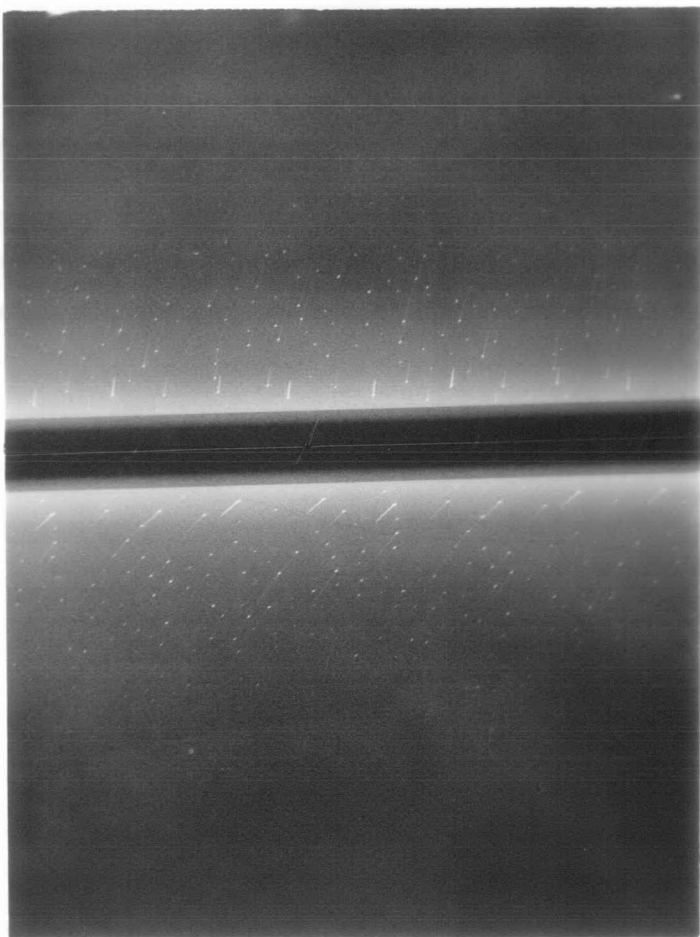
for 200 hours exposure.

Fig. 3.5.2   Weissenberg photograph 1st layer (hkl)
               for 200 hours exposure.

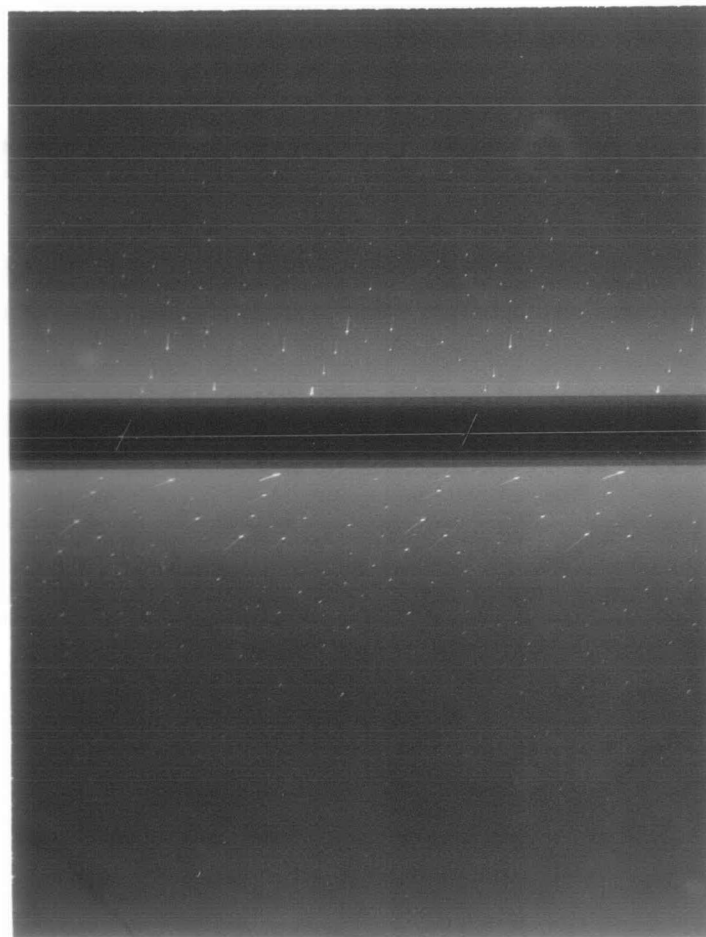

Fig. 3.5.3   Weissenberg photograph 2nd layer (hk2)
               for 200 hours exposure.

Fig. 3.5.4   Weissenberg photograph 3rd layer (hk3)
for 118 hours exposure.

Fig. 3.5.5   Weissenberg photograph 4th layer (hk4)
for 118 hours exposure.

3.6 Powder method

The powder method can be used for a crystalline powder which is composed of fine, randomly oriented particles.

The sample of Nb_3As was oriented randomly to a monochromatic X-ray beam so that the incident ray diffracted by a particular set of planes was deviated by 2θ as shown in Fig.3.6.1, where θ is a Bragg's angle and satisfies Bragg's law

$$n\lambda = 2d \sin\theta$$

The diffracted rays from a plane hkl would generate a cone of semi-apex angle 2θ , as shown in Fig.3.6.2. For a system of randomly oriented crystals, reflected rays from corresponding set of planes will be deviated by 2θ from the direction of the primary beam.

The sample was rotating continuously during the exposure period, and various values of the angle θ about the set of planes were given. The diffraction pattern would be produced by these cones of diffracted rays as they intersect the film. Each line on the film would represent one set of the lattice planes, and the corresponding θ could be obtained from the position of these lines.

The powder photograph for Nb_3As as shown in Fig.3.6.3 was obtained by employing the Guinier-Hägg XDC-700 focusing powder camera using CuK_{α_1} radiation ($\lambda = 1.54051$ Å) at 34 kV, 21 mA. and two-hours exposure. Silicon was used as the internal calibration standard. The general view of the camera and diagram of the principle of the Guinier method were shown in Fig.3.6.4.

If the crystals are small, quite sharp powder lines may be given, but if they are large, the lines tend to be blurred and broadened.

From this powder pattern, the Miller indices of each line and the dimension of the unit cell of Nb_3As were determined.
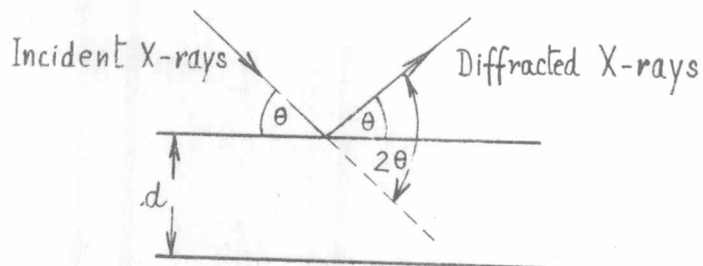

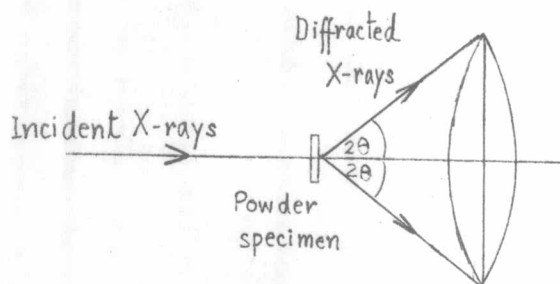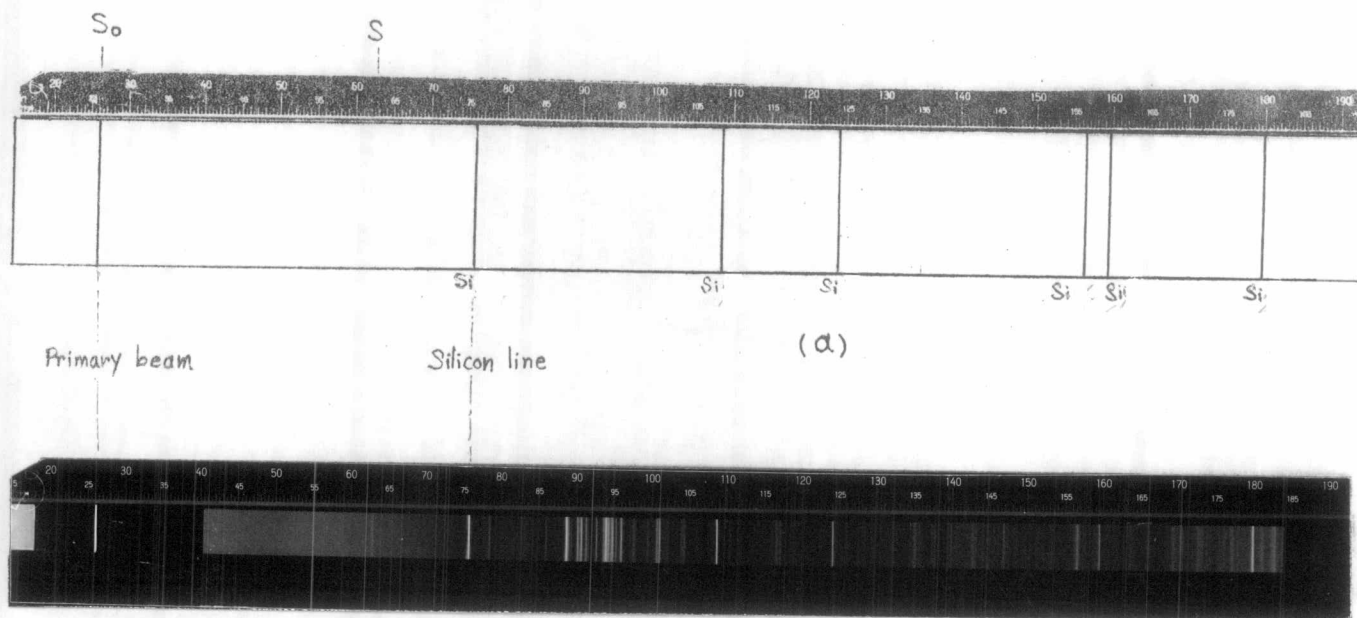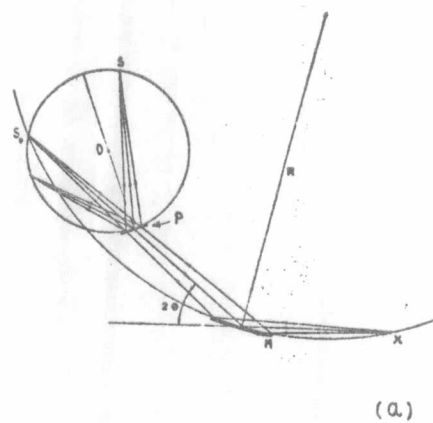Fig.3.6.1 Deviation of 2θ caused by diffraction of X-ray beam.

Fig.3.6.2 A cone of X-rays diffracted by a particular hkl from all the crystallites of a powder specimen.

S_0 S

Si   Si   Si   Si Si   Si

Primary beam   Silicon line   (a)

(b)

Fig.3.6.3 a. A typical diagram of a Guinier-Hägg focusing
              camera photograph.

          b. Powder photograph of Nb_3As. CuK_{α_1} radiation,
              exposed for 2 hours.

X = linefocus of X-ray tube

M = Monochromator

R = radius of monochromator
    focussing circle

P = powder sample

O = center of film cylinder
    in holder

S_o = primary line
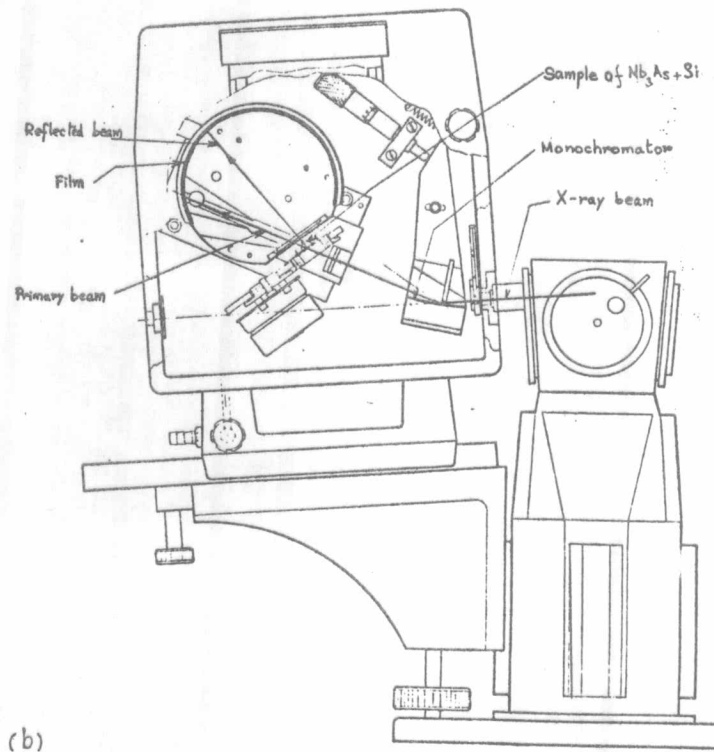
S = reflected line

(a)

(b)

Fig.3.6.4 b. General view of Guinier Hägg camera.

a. Diagram showing the principle of the Guinier
    method.